DEVELOPMENT OF AN ENHANCED ACTIVE POWER CONTROL TECHNIQUE FOR INTERFERENCE MITIGATION IN MACRO-FEMTO CELLULAR NETWORKS

BY

DAWAR, Katfun Philemon
MEng/SEET/2018/7932

DEPARTMENT OF TELECOMMUNICATION ENGINEERING
FEDERAL UNIVERSITY OF TECHNOLOGY, MINNA

NOVEMBER, 2021

ABSTRACT

Femtocells are overlayed on existing Macrocells to form Macro-Femto heterogeneous network (HetNet), to reduce cost of mounting expensive macrocell nodes, improve cellular network capacity and throughput performance. However, HetNet has a major problem of cross-tier and co-tier interference, which hinders its optimal performance, especially when the network capacity expands. With emergence of 5G technologies, interference would become more consequential. Therefore, curbing the effect of this interference is indispensable to sustain larger and efficient HetNet. In this work power control technique was explored to reduce the impact of interference in both Downlink and Uplink scenarios of 5G non-stand-alone (NSA) architecture of Macro-Femto HetNet. An enhanced active power control (EAPC) technique, was developed by hybridizing extended attenuation factor path loss model, Active Power Control (APC), and Power Control 1 (PC1) techniques. Attenuation factor model was extended by adding floor factor to capture both floor attenuation and wall factor, and used same in computing femtocell path loss. The EAPC technique also made use of a different step power value of 0.5 dB for adjusting it's transmit power in order to maximize power and reduce interference. The hybridization when compared with APC and PC1 respectively yielded: 65% and 37% higher Home User Equipment (HUE) throughput; 37% and 21% higher Macro User Equipment (MUE) throughput; 41% and 63% higher throughput of femtocell node (Hen-gNB); 69% and 25% higher throughput of macrocell node (en-gNB). EAPC average power consumption compared to APC and PC1 respectively saved: 65% and 40% HUE battery energy; 38% and 42% MUE battery energy; 54% and 22% Hen-gNB energy. EAPC saved 21% en-gNB energy when compared to APC, but was limited by 8% when compared with PC1.

TABLE OF CONTENTS

LIST OF TABLES

LIST OF FIGURES

LIST OF ABBREVIATIONS

Abbreviation	Meaning
3GPP	Third Generation Partnership Project
4G	Fourth Generation
5G	Fifth Generation
AG	Aggressor
AN	Access Network
APC	Active Power Control
CDF	Cumulative Distributive Function
CQI	Channel Quality Indicator
CSG	Closed Subscriber Group
CSWF	Cross-tier Signal-Link-Plus-Noise-Ratio Based Water Filing
DL-DS	Downlink Desired Signal
DL-IN	Downlink Interference
DPCA	Dynamic Power Control Algorithm
DSL	Digital Subscriber Line
EAPC	Enhanced Active Power Control
EN-DC	Dual Connectivity to Evolved Universal Terrestrial Radio Access Network and New Radio
eNB	evolved Node B
en-gNB	Non-Stand-Alone macrocell logical node
EPC	Evolved Packet Core
E-UTRAN	Evolved Universal Terrestrial Radio Access Network
FAF	Floor Attenuation Factor
FPCT	Fixed Power Control Technique

FUEAPCT	Femtocell User Equipment Assisted Power Control Technique
HeNB	Fourth Generation Femtocell Node
Hen-gNB	Fifth Generation Non-Stand-Alone Femtocell Node
Hen-gNB-GW	Fifth Generation Non-Stand-Alone Femtocell Node Gateway
HetNet	Heterogeneous Network
HP	Hewlett-Packard
HUE	Home User Equipment
ICI	Inter-Cell Interference
IDF	Interference Indication Function
IM	Interference Message
LTE	Long Time Evolution
MME	Mobile Management Entity
MUE	Macro User Equipment
NR	New Radio
NSA	Non-Stand-Alone
PAA	Power Adjustment Algorithm
PC1	Power Control 1
PCID	Physical Cell Identity
PJA	Power Adjustment Algorithm
PLR	Packet Loss Ratio
QIF	Quality of Service Indication Factor
QoS	Quality of Service
S-GW	Serving Gateway
SINR	Signal-to-Interference-plus-Noise-Ratio
SLNR	Signal-to-Leakage-plus-Noise-Ratio

UDN	Ultra Dense Network
UE	User Equipment
UP-DS	Uplink Desired Signal
UP-IN	Uplink Interference
VT	Victim
VoIP	Voice over Internet Protocol

CHAPTER ONE

1.0 INTRODUCTION

1.1 Background to the Study

The cellular communication network is a wireless system where users are clustered into cells and served by nodes. The number of mobile users served by macrocell node is increasing every day, with most of the subscribers located at homes and offices (indoor environment). This indoor mobile user has traffic that comprised of 30% voice and 70% data (Priya and Seema, 2017; Aneeqa, *et al.*, 2017; Onu *et al.*, 2018; Dawar *et al.*, 2021). Indoor propagation path loss is characterized by wall penetration loss, floor attenuation factor, and distance between an indoor node and user equipment. In a homogeneous macrocell network, the cost of mounting several macro nodes to meet up with subscriber's need for high throughput and large coverage is a challenge. This necessitates the deployment of low-power and less expensive nodes to increase the throughput and capacity of the existing macrocell network, at the expense of increase interference.

Interference signals are undesired signals picked by a neighboring receiver, which is a common wireless communication network problem. This interference degrades the performance of the cellular network in terms of drop calls, latency, and poor quality of service; mostly in a partially dedicated channel or co-channel deployment (Priya and Seema 2017). Therefore, there is a need for a thorough study on interference within and between network tiers, in order to develop an efficient interference mitigation technique.

The fifth generation (5G) Ultra-Dense Network (UDN) have a target of increase coverage, throughput, and spectrum efficiency, to accommodate huge subscribers (Agiwal *et al.*, 2016; Asif *et al.*, 2019; Dawar *et al.*, 2021). This can be achieved by

deploying more nodes in a given area, using a large number of small nodes (Farah *et al.*, 2016; Mythili and Mahendran, 2017; Achonu *et al.,* 2020). Femtocell node is the smallest cell node that has high data rate, low latency, easy installation, low energy consumption, better coverage, security, and less packet loss. Researchers asserted that the use of this low-power femtocell on an existing macrocell network to form a heterogeneous network (HetNet) will accomplish the target of wider coverage, high efficiency, and enhanced throughput in the cellular network. (Onu *et al.,* 2018; Amandeep *et al*., 2019; Hassan and Gao, 2019; Haroon *et al*., 2021). However, the expanding installation of femtocells on the existing macrocell network comes with an interference problem. This interference is attributed to the random installation of femtocell nodes by users, and the contention for the same licensed spectrum by both femtocells and macrocells users.

1.2 Statement of the Research Problem

The high demand for voice, data, and video streaming services by an ever-increasing mobile user's mostly located in an indoor environment is alarming (Heli *et al.,* 2015; Tuan, *et al.,* 2017). This is more pronounced with the increase in virtual meetings, telemedicine, smart agriculture, smart city, smart homes, and cloud computing. Ericsson's mobility report, as presented in Sajjad *et al.* (2018), indicated that in 2021, there will be nine billion mobile broadband subscriptions, out of which seven billion will use mobile data. Their report also pointed out, that smartphone data will increase by 20% and video traffic will increase by 25%. As the demands increase with the advent of 5G Ultra-Dense Network, the cell coverage, network capacity and throughput of homogeneous network will reduce, resulting into poor indoor network services.

According to literatures, the overlay of femtocell on existing macrocell netwok is said to be one of the promising technique that would provide the needed solution to the poor indoor network service, increased network coverage and capacity (Heli *et al*., 2015; Xu and Qui, 2018). However, femtocell node being a plug and play node, that used license frequency band, and is installed by subscribers without taking into cognizance its cell coverage or other nearby cells, have high chances of cell overlap, that causes an increase in interference. This interference is the main technical problem attributed with Macro-Femto HetNet (Al-omari *et al.*, 2016; Farah *et al.*, 2016; Feng, *et al*., 2018; Mohammad *et al*., 2019).

Researchers have postulated different power control techniques for curbing the interference problem with successes, even though there is still room for improvement. This research seeks to study interference in Macro-Femto HetNet and developed an enhanced power control technique from existing power control techniques; to contribute in solving the interference problem in Macro-Femto HetNet.

1.3 Aim and Objectives of the Research

The research aims at developing an Enhanced Active Power Control (EAPC) technique for interference mitigation in 5G Non-Stand-Alone (NSA) architecture of Macro-Femto cellular communication networks. To achieve this, the following objectives were set:

i. Hybridization of attenuation factor model, active power control technique and power control 1 techniques to develop an enhanced active power control (EAPC) technique.
ii. Simulate EAPC technique in Macro-Femto cellular communication network using MATLAB.

iii. To evaluate the performance of the EAPC technique and compare it with that of existing power control techniques, in terms of throughput and power consumption.

1.4 Scope of the Study

The research work centred on developing an enhanced active power control technique, for mitigating co-tier and cross-tier interference in 5G NSA of Macro-Femto HetNet. The research system architecture, parameters, and assumptions would guide the MATLAB simulation of the Macro-Femto HetNet. The performance of the EAPC technique would be compared with that of PC1 and APC technique in terms of throughput and transmit power consumption.

1.5 Justification for the Study

Interference is a major problem in wireless communication networks which reduced network throughput and increase drop calls.

The work of Hassan and Gao (2019) proposed an active power control technique for mitigating interference in Macro-Femto communication networks, which reduced interference in the network, gave high throughput and low node power consumption when benchmarked; but more need to be done to improve on the existing technique. Their network scenario considered static user equipment (UE) and cross-tier interference only; it did not considered co-tier interference and attenuation due to floor. Therefore there is a need to enhanced active power control technique, consider co-tier and cross-tier interference, attenuation due to floor factor, and mobile UEs to capture a realistic network scenario, further reduce power consumption and increase network throughput in 5G Macro-Femto communication networks.

1.6 Thesis Outline

The remaining part of the thesis is organized as follows. Chapter two review 5G non-stand-alone architecture, femtocell network, femtocell access mode, Macro-Femto HetNet, network interference in Macro-Femto HetNet, mathematical models for Macro-Femto HetNet, and also related works of literature on interference mitigation using power control technique. Chapter three presents the research system model, and methodology. Chapter four presents and discusses the MATLAB simulation results in sections. And chapter five states the conclusion and recommendations of the research.

CHAPTER TWO

2.0 LITERATURE REVIEW

2.1 Preamble

The rapid increase of smartphones and the growth of multimedia services with more mobile data and voice traffic emanating from indoor environments where the coverage of macrocell is not good enough is a problem in cellular communication. Researchers postulated in several works of literature the use of femtocell to curb the challenge of network coverage and throughput when interference is efficiently mitigated. This interference problem can be reduced using diverse mitigation techniques, such as power control, frequency reuse, and cognitive radio sensing technique, but cannot be eliminated completely. This research work centered on mitigating interference using power control technique, because of its merits which include: universal frequency reuse, transmit power utilization, and simplicity. The chapter presents a review on 5G non-stand-alone (NSA) architecture, femtocell network, HetNet, types of Macro-Femto interference, mathematical models, and related power control techniques for interference mitigation.

2.2 Fifth Generation (5G) Non-Stand-Alone (NSA) Architecture

5G Mobile Systems (5GS) introduced a New Radio (NR) and interfaces that provide the required technology to support different types of services. 5GS has two architectures; the 5G Non-Stand-Alone (NSA) and 5G Stand-Alone (SA). In the 5G SA architecture, 5G user equipment communicates to the new 5G Access Network (AN), which in turn connects to the new 5G Core Network only (3rd Generation Partnership Project “3GPP” release. 15.0.0; Imane *et al*., 2020).

NSA architecture is a step toward full 5G implementation. The AN and NR interface of 5G NSA is compatible with 4G Long Time Evolution (LTE) node and its Evolved Packet Core (EPC) infrastructure. This makes 5G NSA NR technology accessible to 4G LTE users without replacing the 4G core network infrastructures. Figure 2.1 shows an illustration of 5G NSA architecture.

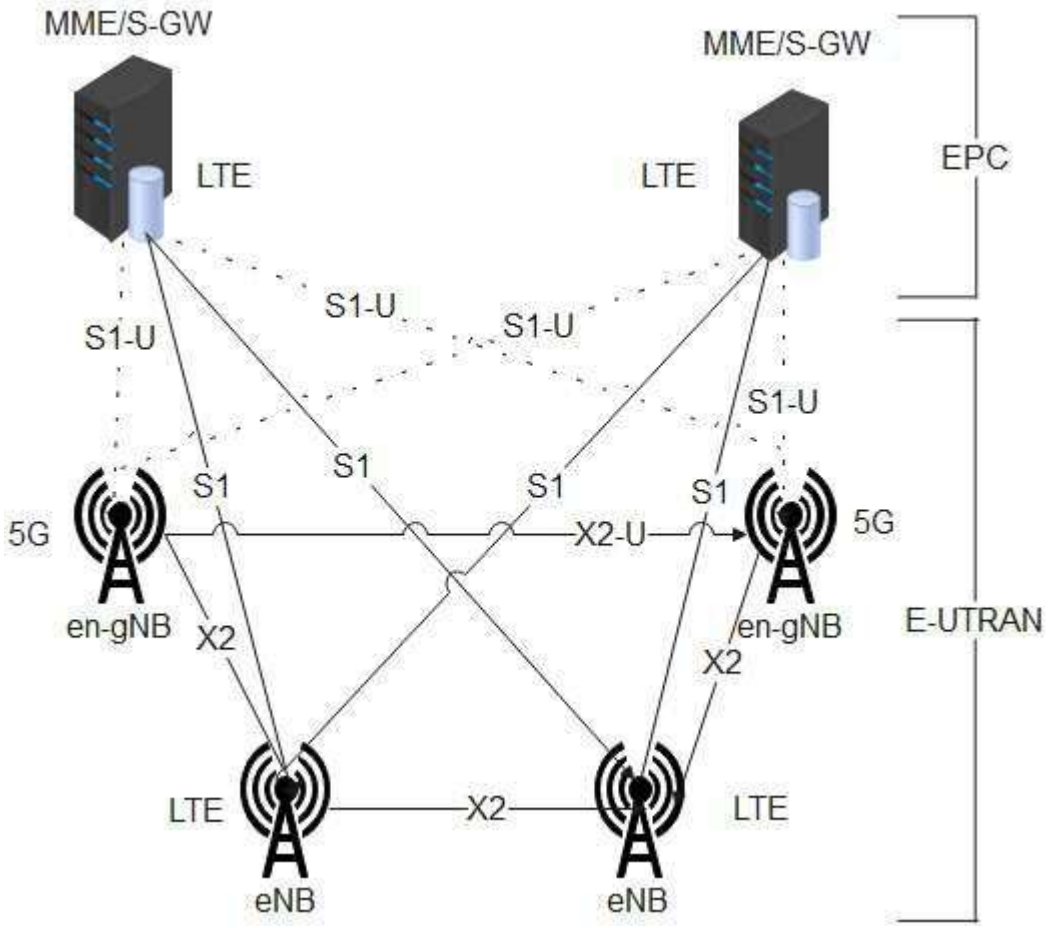

Figure 2.1: 5G NSA architecture

(Source: 3GPP Release 15.0.0)

According to the architecture of 5G NSA, the NR node (logical node "en-gNB") connects to 4G LTE node (logical node "eNB") using an X2 interface. The en-gNBs connect each other via the X2-U interface and connects to EPC using the S1-U interface. In NSA, 5G handles the U-Plane, that has to do with data packets; while the C-plane that has to do

with control signals for call origination and termination, UE location and registration, are handled by the LTE eNB and EPC (Imane *et al*., 2019). The NSA is also called “EN-DC", for "E-UTRAN and NR Dual Connectivity” because it connects both 4G AN (E-UTRAN) and 5G AN (3rd Generation Partnership Project “3GPP” release 15.0.0; Imane *et al*., 2019).

2.3 Femtocell Network

Femtocell network from the prefix femto is a very small cellular network, refer to as a home network. The femtocell node (Hen-gNB) is a very small access point that has low transmit power, low cost, and is installed by users. It has a cell coverage radius of 20 – 30m (Adeyemo *et al.,* 2015; Onu *et al*., 2018; Haroon *et al*., 2019). The femtocell connects user equipment to core network of mobile operator's using residential Digital Subscriber Line (DSL) backhaul, cable broadband, or fiber cable. The major benefit of femtocell network is an increase in system throughput when interference is well mitigated (Gurpreet *et al.,* 2016; Jundhare and Kulkarni, 2016; Priya and Seema 2017). Femtocell interference problem is characterized by uncertainty in the position of Hen-gNBs, irregular cell coverage, co-channel deployment, and Hen-gNB access mode (Jinlong *et al.*, 2015; Priya and Seema, 2017).

The 4G LTE-5G NSA architecture of femtocell is divided into two main segments. EPC and the enhanced universal terrestrial radio access network (E- UTRAN). The E-UTRAN is made up of femtocell nodes. While, the EPC consists of femtocell–gateway (Hen-gNB - GW), mobile management entity (MME), and serving gateway (S-GW). Figure 2.2 presents a schematic diagram of a typical 4G–5G NSA femtocell network.

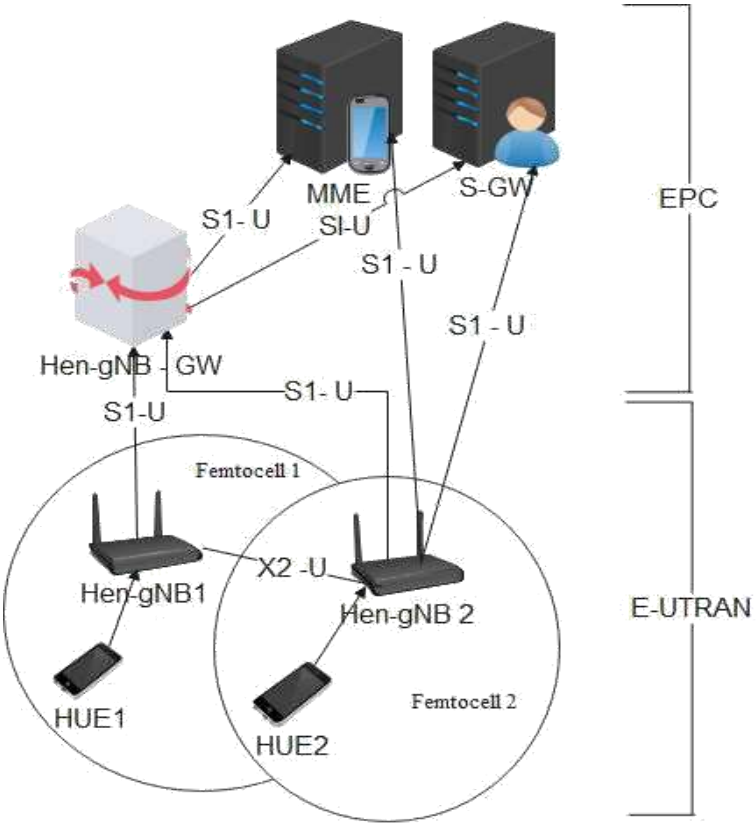

Figure 2.2: Femtocell network

(Source: 3GPP release 15.00; Asif, *et al.*, 2019)

From Figure 2.2, HUE 1 stand for Home User Equipment (HUE) 1 of femtocell 1, HUE 2 stand for HUE 2 of femtocell 2. According to the 3GPP standard, femtocell node transfer information directly to MME and serving gateway (S-GW) using S1-U interface or optionally through Hen-gNB gateway (Hen-gNB-GW). The Hen-gNB-GW communicates with MME and S-GW through S1-U interface. It is responsible for aggregating a large number of connected Hen-gNBs, and connects them to a core network. MME helps to authenticate UEs, pages UEs, and tracks both active and idle UEs. S-GW routes and forwards user data packets and terminate downlink data for idle UEs. It also hold packets send to an idle UE until the idle UE is paged and a Radio Frequency (RF) channel is re-established. The S-GW is also responsible for Internet protocol backhaul admission and congestion control.

2.3.1 Femtocell access mode

The ability of UE to access Hen-gNB services can be restricted or unrestricted, this forms the basis for the three femtocell access modes, which are: open, closed, and hybrid (Sharanya *et al.,* 2015; Tarte and Hanchate, 2017; Hassan and Gao, 2019). Open access mode allows all UEs to connect to any close by Hen-gNB without any restriction or permission. HUE connects to an open access Hen-gNB whenever it receives a high signal from the nearby Hen-gNB. Closed access mode which is also called Closed Subscriber Group (CSG), is a restricted access mode that allows only registered UEs on a particular Hen-gNB to connect and use its services. Whereas, the hybrid access mode is a combination of open and closed access mode, where registered HUEs are given higher priority when compared to unregistered HUE. The registered HUEs have a large portion of reserved transmission bandwidth for their usage, while the unregistered HUEs contend for the remaining small transmission bandwidth.

2.4 Macro-Femto Heterogeneous Network

The Macro-Femto heterogeneous network is a two tiers cellular communication network that comprises of macrocell and femtocell networks, co-existing together to expand network coverage, and increase throughput performance (Afolalu *et al*., 2016; Achonu *et al*., 2017)**.** There are other different types of small cell networks that can be integrated into existing macrocell network; examples of such small cell networks are microcell, and picocell (Meer and Kaleem 2020). Among the different small cell networks, femtocell have been the most promising, in terms of high quality of service to indoor users, low cost to network providers, and easy installation (Andrian *et al*. 2015; Xuan *et al.,* 2016; Haroon *et al.,* 2019). Figure 2.3 gives a schematic diagram of Macro-Femto HetNet.

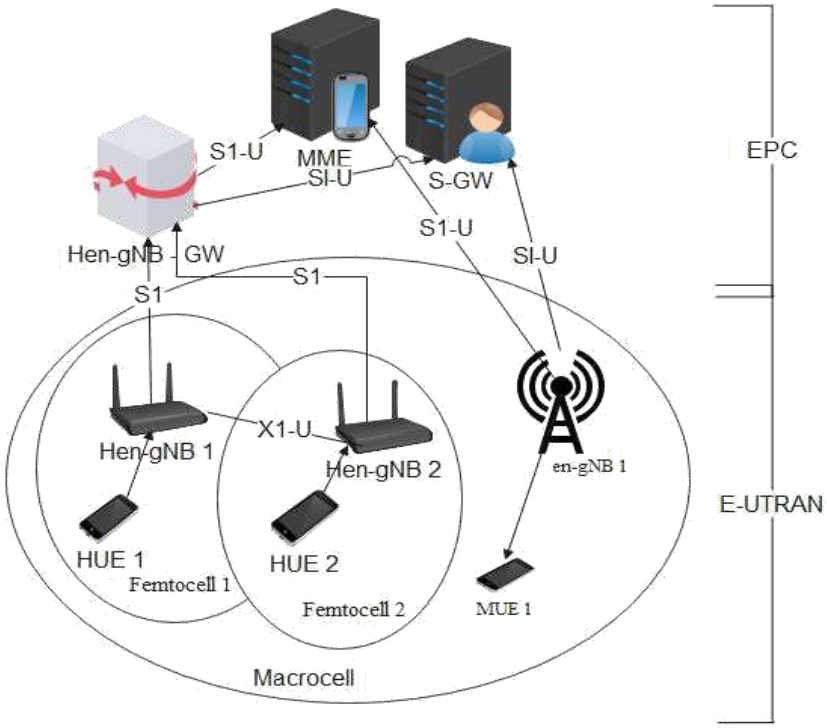

Figure 2.3: Macro-Femto heterogeneous network architecture

(Source: 3GPP release 15.0.0; Feng *et al*., 2018; Asif, *et al*., 2019)

2.5 Macro-Femto Interference

According to Achonu *et al.* (2020), interference greatly affects the performance and quality of service of 5G network. Macro-Femto interference largely depends on the type of channel deployment used in a particular cellular network. A channel deployment is said to be fully dedicated when the bandwidth is not shared by different network tiers; hence, there will be no cross-tier interference, a tradeoff for bandwidth utilization. In partial dedicated channel deployment, part of the available bandwidth is assigned only to macro user equipment (MUE), and the remaining part is shared by MUE and HUE. While in co-channel deployment the entire available bandwidth is used by both MUE and HUE simultaneously. Interference is more pronounced in Macro-Femto HetNet when co-channel deployment and femtocells closed access mode are considered (Sharanya *et al.*, 2015; Hassan *et al*., 2018).

The works of Andrian *et al*. (2015); Syed and Aashish (2017); and Tuan *et al.* (2017) classified interference into cross-tier and co-tier interference based on aggressor (AG) and victim (VT) tier. Co-tier interference occurs among network devices that belong to the same tier. While Cross-tier interference occurs when devices in different network tiers share the same spectrum. Co-tier and cross-tier interference are subdivided into uplink co-tier, uplink cross-tier, downlink co-tier, and downlink cross-tier interference, as illustrated in Figure 2.4.

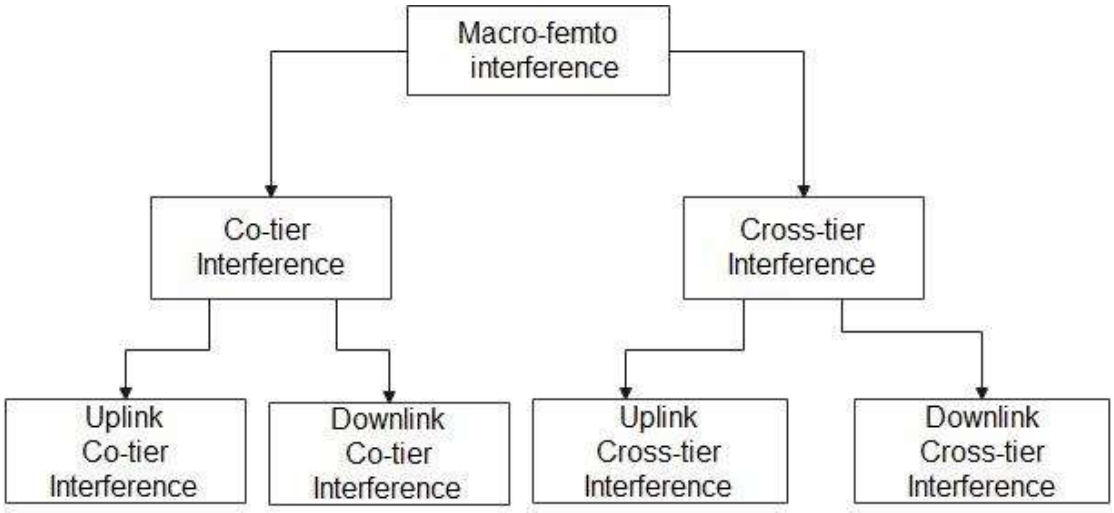

Figure 2.4: Types of interference in Macro-Femto heterogeneous network

(Source: Andrian *et al*., 2015; Syed and Aashish 2017; Tuan *et al.*, 2017)

2.5.1 Uplink co-tier interference

The uplink transmission, of HUE or MUE, causes uplink co-tier interference to nearby Hen-gNB or en-gNB, respectively, as illustrated in Figure 2.5.

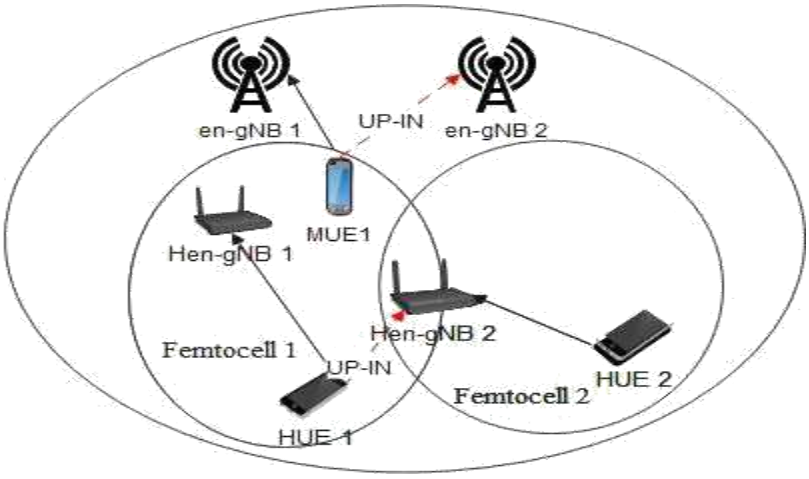

Figure 2.5: Uplink co-tier interference in Macro-Femto heterogeneous network

(Source: Syed and Aashish 2017; Tuan *et al.*, 2017)

In Figure 2.5, Hen-gNB 1 and Hen-gNB 2 stand for femtocell node in cells 1 and 2 respectively. UP-IN stands for uplink co-tier interference signal. The uplink transmission of HUE 1 from femtocell 1 is received by nearby Hen-gNB 2 from cell 2 as an uplink co-tier interference, in which HUE 1 is the AG and Hen-gNB 2 is the VT. The uplink transmission of MUE 1 communicating to en-gNB 1 is received by nearby en-gNB 2 as an uplink co-tier interference, whereby MUE 1 is the AG and en-gNB 2 is the VT.

2.5.2 Downlink co-tier interference

Downlink transmission of Hen-gNBs or en-gNBs are received by nearby HUEs or MUEs respectively as downlink co-tier interference. In such circumstances, Hen-gNBs and en-gNBs are AGs, while HUEs and MUEs are VTs. Figure 2.6 shows an illustration of downlink co-tier interference.

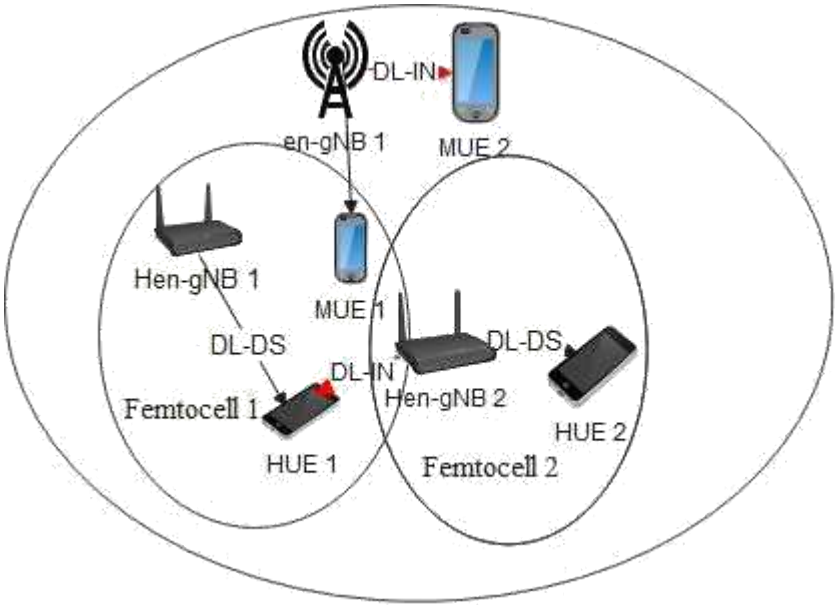

Figure 2.6: Downlink Co-tier interference in Macro-Femto heterogeneous network

(Source: Syed and Aashish 2017; Tuan *et al.*, 2017)

In Figure 2.6, DL-DS stands for downlink desired signal, DL-IN stands for downlink co-tier interference signal. The downlink transmission of Hen-gNB 2 in femtocell 2 is received by nearby HUE 1 in femtocell 1 as downlink co-tier interference; whereby Hen-gNB 2 is the AG and HUE 1 is the VT. The downlink transmission of en-gNB 1 is received by nearby MUE 2 as downlink co-tier interference; where en-gNB 1 is the AG and MUE 2 is the VT.

2.5.3 Uplink cross-tier interference

The uplink transmission of HUEs and MUEs are the source of cross-tier interference to nearby en-gNB and Hen-gNB, respectively. Figure 2.7 illustrates uplink cross-tier interference.

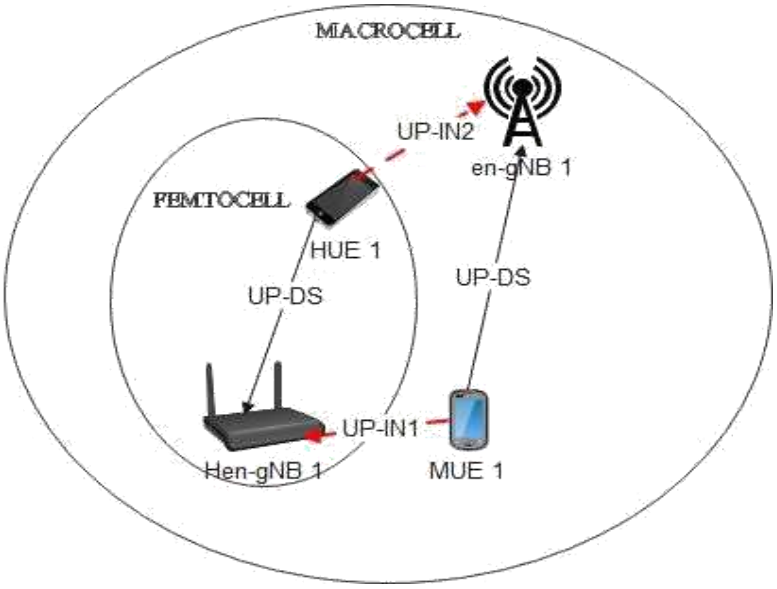

Figure 2.7: Uplink cross-tier interference in Macro–Femto heterogeneous network

(Source: Syed and Aashish 2017; Tuan *et al.*, 2017)

In Figure 2.7, UP-DS stands for desired uplink signals, UP-IN1 stands for uplink cross-tier interference where MUE 1 is the AG and Hen-gNB 1 is the VT. Also UP-IN2 is an uplink cross-tier interference where HUE 1 is the AG and en-gNB 1 is the VT.

2.5.4 Downlink cross-tier interference

The downlink transmission of en-gNB and Hen-gNB in a network causes downlink cross-tier interference to nearby HUEs and MUEs, respectively. Figure 2.8 presents an illustration of cross-tier interference in a typical Macro-Femto HetNet.

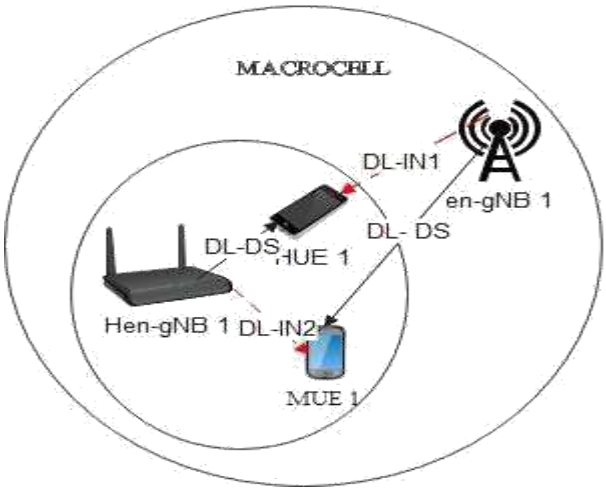

Figure 2.8: Downlink cross-tier interference in Macro-Femto heterogeneous network (Source: Syed and Aashish 2017; Tuan *et al.*, 2017)

In Figure 2.8, DL-IN1 stands for downlink cross-tier interference where en-gNB 1 is the AG and HUE 1 is the VT. DL-IN2 stands for downlink cross-tier interference where Hen-gNB 1 is the AG and MUE 1 is the VT.

2.6 Mathematical Models

Mathematical models are description of systems using mathematical concepts and language. The analytical computation of path loss, signal-to-interference-plus noise ratio (SINR), and throughput, are all carried out using different mathematical models.

2.6.1 Log-distance path loss model

The log-distance path loss model is an analytical approach, which was derived from Friis free space model. The propagation path loss experience in a radio propagation channel between a transmitter and receiver can be expressed as a function of distance by using a path loss exponent (n) that depends on the type of environment Rappaport (2002). The

general path loss model, which is referred to as log-distance Path Loss (PL) model is presented in equation (2.1).

$$\propto \left(\quad \right) \tag{2.1}$$

The log-distance path loss model in decibel PL (dB) at an arbitrary distance > 0 is given in equation (2.2).

$$( ) = (0)[ ] + 10 \quad (\quad) \tag{2.2}$$

The value of path loss at reference distance of $_0$ ($_0$) is obtained using Friis path loss as expressed in equation (2.3) or by field measurement at $_0$. Equation (2.1), (2.2), and (2.3) were all sourced from Rappaport (2002).

$$(0)[ ] = -10 \left(\frac{2}{4} \right) \tag{2.3}$$

where is the wavelength of the signal, is pie, is path loss exponent, $_0$ is the close-in or reference distance, that ranges from 1 – 10m in an indoor propagation, d is the distance between the transmitter and the receiver and ($_0$) is reference path loss due to reference distance $_0$. Table 2.1 presents a summary of path loss exponent range based on the different environments.

Table 2.1: Path loss exponent of different environments

S/N	Environment	Path loss exponent (n)
1.	Free space	2
2.	Urban area cellular radio	2.7 - 3.5
3.	Shadowed urban cellular radio	3 – 5
4.	In building line-of-sight	1.6 - 1.8
5.	Obstructed in building	4 – 6
6.	Obstructed in factories	2 – 3

(Source: Rappaport, 2002)

2.6.2 Attenuation factor model

Attenuation factor model is an indoor propagation model that was derived from log-distance path loss model, by adding floor attenuation factor ( ) to log-distance model. The attenuation factor model as presented in Rappaport (2002) is given in equation (2.4).

[( )] = [( )] + 10 ( ) + (2.4)

where [( )] is log-distance path loss from transmitter to receiver, [( )] is free space path loss, is path loss exponent, stands for close-in reference distance, is the distance between transmitter and receiver, and is floor attenuation factor.

2.6.3 Signal-to-interference-plus-noise ratio

Signal-to-Interference-plus-Noise Ratio (SINR) is used in wireless communication, which is similar to Signal-Noise Ratio (SNR) in wired communication. The SINR is defined as particular signal power received divide by interference power and noise in the communication system. When the background noise in the system is zero, then SINR becomes Signal-to-Interference Ratio (SIR). SINR is mathematical expressed in equation (2.5).

= (2.5)

where is the SINR of receiver *x,* is the power of received desired signal, and ∑ is the sum of all interference in the wireless network.

2.6.4 Cumulative distribution function

The cumulative distribution function (CDF) of a real-valued random variable *X* is a function expressed in equation (2.6) (Deisenroth *et al*., 2020).

$$()=(\leq) \tag{2.6}$$

where ( ) is the probability that the random variable *X* takes on a value less than or equal to *x*. The probability that the random variable *X* lies in the semi-closed interval (a, b), where a < b, is therefore given in equation (2.7).

$$(< \leq) = ( ) - ( ) \tag{2.7}$$

The CDF of a continuous random variable *X* can be expressed as the integral of its probability density ( ) as given in equation (2.8).

$$() = \int_{-\infty}^{} () \tag{2.8}$$

2.7 Floor Attenuation Factor

In indoor system propagation, floor causes loss in signal strength, referred to as floor attenuation factor. The value of floor attenuation factor varies, due to materials used in constructing the floor within the same and different floors of a building. The Floor Attenuation Factor (FAF) for one, two, three, and four floors in two office buildings as presented in Rappaport (2002) is captured in Table 2.2.

Table 2.2: Total floor attenuation factors in office buildings

Building	FAF (dB)
Through One Floor	16.2
Through Two Floors	27.5
Through Three Floors	31.6

(Source: Rappaport 2002)

2.8 Related Power Control Techniques

Power is one of the limited resources in mobile networks; which if not properly manage will cause significant increase in interference. Hence, the need for UEs and nodes to transmit with the required power that can guaranty a good link quality.

2.8.1 An active power control technique

Hassan and Gao (2019) worked on addressing interference problem in Macro-Femto HetNet to maximize high data rate for indoor mobile users; using proposed Active Power Control (APC) technique. Their system model considered downlink transmission of Macro-Femto HetNet, one macrocell, one femtocell configured in closed access mode.

In APC the transmit power of AG is adjusted based on received Interference Message (IM). The VT of interference compute Interference Indication Function (IDF) and compared it with set IDF threshold to determine whether to send an IM or not. When the computed IDF is greater than the set threshold interference, the VT send an IM that contained the AG information to its transmitter, which then forwards the IM using backhaul link to the AG; otherwise it does not send an IM. Equation (2.9) presents the mathematical equation for computing IDF, and equation (2.10) expresses mathematically when IM is sent or not.

(2.9)

(2.10)

where stands for IDF, stands for transmitting power, stands for log – normal shadowing, and ( )$^{-}$ represents the path loss component for the indoor transmission. In equation (2.10), stands for IM, and h h stands for set interference threshold. When $= 0$, there is no interference and IM is not sent, but when $= 1$, it implies there is interference and IM is sent. The APC technique has two power adjustment stages: the first stage, set three transmit power (, ,), where was their maximum,

followed by and lastly as the minimum transmit powers. Also, the APC technique considered two-time levels (1, 2). First phase of APC power adjustment would activate whenever an IM is received. On receiving an IM, the transmit power of the AG 20

would change from to by downward step power value (Δ). If the same AG

receives another IM within the first time level (1), it would not further reduce its power to level until 1 expires. Similarly, when the AG has no IM and 1 expired, then the second time level (2) starts and the next transmit power level would increase from to by upward step power value (Δ). The value of Δ and Δ steps power

were both set to 2 dB. The mathematically expression used for adjusting the first stage, APC transmit power is captured in equations (2.11) – (2.15).

- No interference message (2.11)

= = − Δ Interference Message and 1 starts (2.12)

- - − Δ New interference Message and 1 starts (2.13)

- - + Δ No interference Message and 2 starts (2.14)

- - + Δ No interference Message and 2 running (2.15)

where is APC first stage transmit power. The second stage of active power control technique shapes was based on first stage power value and the minimum required Quality of Service (QoS) for received signal. The mathematical model for computing the QoS Indication Function (QIF) is presented in equation (2.16).

QIF = ——— (2.16)

where is the reference signal transmit power, is the minimum required signal-to-interference-plus-noise ratio (SINR) for HUE, and is the reference

signal received power. The second and final stage of APC transmit power ( ) is expressed mathematically in equation (2.17) and the path loss models used are equation (2.18) and (2.19).

= max((∗ .)) (2.17)

where and are minimum and maximum transmit power respectively, and is the second stage transmit power, known as APC transmit power.

15.3 + 37.6 10( ) ( )
=1 (2.18)
15.3 + 37.6 10( ) + ( )

38.46 + 20 10(2) ( )
=1

max (15.3 + 37.6 10(2), 38.46 + 20 10(2)) + ( )

(2.19)

Where stands for propagation path loss when a macrocell node is transmitting to its receiver, is propagation path loss when a femtocell node is transmitting to its receiver. is the distance from the macrocell node to its user equipment, $_2$ is the distance between the femtocell node and its user equipment. is wall penetration loss.

Equations (2.9) – (2.19) were all sources from (Hassan and Gao, 2019).

The simulation result in their work indicated that APC reduces Inter-Cell Interference (ICI) and had better MUE throughput compared to Fixed Power Control technique (FPCT), Femtocell User Equipment Assisted Power Control Technique (FUEAPCT) and macrocell User Equipment Assisted Power Control Technique (MUEAPCT).

2.8.2 An adaptive network sensing power control technique

Hassan *et al*. (2018) work, titled interference management in femtocells by the adaptive network sensing power control technique, contributed in solving the problem of ICI in downlink transmission of Macro-Femto HetNet. Their system model considered a cross-tier interference scenario where the MUE computed received IDF and compared it with set value of interference threshold. If the computed IDF is greater than the interference threshold value, the MUE would send a message to its node that contains

information of the interfering femtocell node. They computed IDF and IM using equations (2.9) and (2.10). Equation (2.18) and (2.19) were used for computing path loss. They adjusted their femtocell transmit power using equation (2.20) and (2.21).

$$ - \quad - \quad + \ (1) \tag{2.20}$$

$$= \max(\ \min(\ ,)) \tag{2.21}$$

where is macrocell power, – is macrocell to femtocell path loss, (1) is the line of sight (LOS) path loss with cell range of 1, and is the adaptive network sensing power.

The simulation result of ANS indicated that the proposed technique when compared to FUEAPCT, MUEAPCT, and FPCT gave a better MUE throughput, and decrease in HUE throughput.

2.8.3 Dynamic power control technique

The work of Susanto *et al.* (2017)[a], titled downlink power control for interference management in Femtocell-Macrocell cellular communication network, was tailored towards solving the interference problem in downlink Femtocell – Macrocell cellular communication network. They used a power control approach called power control 1 (PC1) technique to mitigate the interference problem in Femtocell – Macrocell network.

In PC1, the transmit power of en-gNBs and Hen-gNBs were adjusted based on interference received by UE. The difference between computed UE SINR ( ) and target SINR ( ) was used to determine interference in the

two-tier network. The difference between measured SINR and target SINR is expressed mathematically in equation (2.22).

=−

(2.22)

When the computed SINR is less than the target SINR, the next transmit power of en-gNB, or Hen-gNB, would be increased by 2 dB. When the computed SINR is greater than the target SINR, the next transmit power of en-gNB, or Hen-gNB would be decreased by 2 dB. When the computed SINR is equal to the target SINR (SINR),

the next transmit power of en-gNB, or Hen-gNB would be the present transmit power.

Mathematically, the PC1 transmit power adjustment is expressed in equation (2.23).

$$( ) = \begin{cases} \min[\ ( ) + \Delta\ ,\ \ ]; & \leq 0 \\ \max[\ ( ) - \Delta\ ,\ \ ]; & > 0 \end{cases} \quad (2.23)$$

Δ Δ stand for

where and step power values used to increase and reduce next transmission power respectively. ( ) is the current transmit power and ( ) is the

next transmit power. The mathematical equations used for computing macrocell and femtocell path loss are presented in equation (2.18) and (2.24) respectively.

$$( ) = 127 + 30 \quad \left(\frac{\ }{1000}\right) \quad (2.24)$$

where 1_( ) stand for the propagation path loss in femtocell network. Their result was plotted in terms of Cumulative Distribution Function (CDF) of SINR, where the proposed PC1 technique outperformed that of no power control.

The work of Susanto *et al*. (2017)[b], titled interference management using power control for uplink transmission in Femtocell-Macrocell Cellular Communication used same PC1 technique to mitigate interference problem in uplink transmission of Femtocell-Macrocell network. The result obtained indicated that PC1 technique outperformed when there is no power control in terms of CDF of SINR.

2.8.4 An interference mitigation scheme for LTE based femtocell networks

Ali *et al.* (2016) work, titled an interference mitigation scheme for LTE based femtocell networks considered only co-tier interference. The work pointed out interference as the major challenge of femtocell network which it seeks to address using proposed technique. Their proposed interference mitigation technique had two parts: the self-configuration and self-optimization part. In the self-configuration stage, the femtocells boots and automatically start transmitting with maximum transmit power. While in the self-optimization stage, the initialized femtocell checked, if there was a neighboring femtocell. In a situation where there was at least one neighboring femtocell, the femtocell would be switched to Transmit Power Control Mode (TPCM) and adjust its next transmit power to reduce interference on the neighboring femtocell. Otherwise, it continue to transmit with maximum power.

The results of video and Voice over Internet protocol (VoIP) Packet Loss Ratio (PLR) using TPCM were both lower compared to static power approach. The average throughput of video and VoIP flow was better compare to static power approach; it also showed that as the number of femtocells in the network increases, the throughput decreases.

2.8.5 Cross-tier signal-leak-noise-ratio based water filling power allocation algorithm

Su *et al.* (2016) work titled power allocation scheme for femto-to-macro downlink interference reduction for smart devices in ambient intelligence, was geared towards using power allocation technique to solve the problem of cross-tier interference in closed access mode femtocells. It centered on allocating Physical Resource Block (PRB) power

of 4G femtocell node (HeNB), based on modified water filing power algorithm; called cross-tier signal-to-leakage-plus-noise ratio (SLNR) based water filling (CSWF). Where the CSWF method generate the water bottom (,). The water bottom is defined mathematically in equation (2.25).

$$\Sigma \quad + \qquad (2.25)$$

where Σ stands for the total of interference on HUE, for thermal noise per PRB, and , for channel gain of PRB between HeNB f and HUE . The transmit power of a HeNB f at PRB ( ), is determined where is a set water level. The mathematically expression of is presented in equation (2.26).

$$\begin{cases} - \ , & < 0 \\ 0, & \geq 0 \end{cases} \qquad (2.26)$$

The path loss model they used for macrocell and femtocell networks is given in equation (2.18) and (2.19) respectively. Their result indicated that CSWF technique had better MUE throughput compared to when their no power management; as a tradeoff for HUE throughput, which decreased by 1.1%.

2.8.6 Dynamic power control algorithm

Xuan *et al.* (2016) work, titled dynamic power control for maximizing system throughput in enterprise femtocell networks, used a Dynamic Power Control Algorithm (DPCA) for femtocell nodes (HeNBs) to solve the problem of system throughput in a centralized network. The HeNBs applied the DPCA algorithm in a distributed manner. Where HeNB adjusted it's transmit power based on the transmit power of neighboring HeNB or received SINR of HUE. Their system model considered cross-tier interference,

co-channel deployment, multiple HUEs, and HeNBs. The DPCA was in two phases: the permission judgment algorithm (PJA) and power adjustment algorithm (PAA).

A HeNB has a list of all its neighboring HeNBs and their transmitting power. During the PJA, the HeNB listened to the network for any change in transmit power of any adjacent neighbor; where there is change, it would not adjust its transmit power, and when there is no change, it would then move into the second phase of the algorithm to adjust it transmit power. All non-adjacent neighbors can adjust their power giving rise to multiple femtocells performing dynamic power control in a distributed manner.

The PAA has two modules, the non-periodic with the highest priority and the periodic modules. The periodic module is activated by PJA, while the non-periodic module is activated when UE(s) at a distance ( ) needs to be handover to another HeNB or the received HUE SINR is less than the set HUE SINR threshold value. The new transmit power is adjusted using the mathematical expression in equation (2.27) and (2.28).

$$= (\quad) \quad \times \tag{2.27}$$

$$= (\quad \leq \tag{2.28}$$

where is path loss of indoor transmission, is the old transmit power, is old cell radius is new cell radius and is maximum HeNB radius with maximum transmit power. The path loss model they used within femtocell network is captured in equation (2.29).

$$( ) = 38.5 + 20 \quad 10(\ 2) \tag{2.29}$$

The result of using the proposed DPCA power control technique gave a 40% improvement in system throughput when compared to when their no power control.

2.8.7 Stochastic approximation algorithm

Haining *et al.* (2015) work, titled femtocell power control for interference management based on macro-layer feedback used stochastic approximation algorithm for downlink power control in femtocell networks to solve the problem of cross-tier interference in Macro-Femto network. Stochastic approximation (SA) algorithm is a distributed femtocell node power control approach for managing interference in a Macro-Femto network. The system model they used had one macrocell, femtocell nodes, fixed MUE and HUE.

During downlink transmission, HeNB does not received feedback from eNB or communicate with MUE directly, rather it listens to feedback that was send from interfered MUE to its serving eNB. When HeNB overheard the feedback sent by MUE, it knows that it is causing interference to MUE and thereby reducing it's transmit power using a stochastic algorithm. This work did not spell out the propagation path loss model used.

2.8.8 Dynamic power tuning technique

Sharanya *et al.* (2015), work titled dynamic power tuning for downlink interference mitigation in heterogeneous LTE network aimed at solving cross-tier interference in uplink, downlink transmission of Macro-Femto HetNet using proposed dynamic power tuning technique.

In dynamic power tuning technique, when a MUE received an interference signal from HeNB, it will send the reference signal received power with the corresponding physical cell identity (PCID) of the AG and channel quality indicator (CQI) message to its serving

eNB. The eNB determined the femtocell causing the interference and sends an IM back to its MUE, which then forwards the interference message to the interfering HeNB. When the AG received the interference message it reduces its transmit power based on the number of HUEs within its cell. If the number of HUEs in the interfering HeNB is greater than one, the HeNB would reduce its current transmit power by 4 dBm in the next transmission, and if the number of HUE is exactly one the HeNB will reduce it's transmit power to 10 dBm.

Results they obtained shows that the proposed dynamic power tuning technique reduced interference to MUE when compared to dynamic power allocation and HUE based power control techniques, and HeNB had low transmission power when compared to dynamic power allocation and HUE based power control techniques.

2.9 Research Gap

The active power control technique used in the work of Hassan and Gao 2019 gave better throughput and low power consumption when compared with MUE assisted power control and HUE assisted power control techniques. However, their work did not consider co-tier interference and the method used in determining interference was complex, having several equations and parameters. The complexity and second stage of computing their node transmit power will result into increase processing delay and high memory requirement due to many variables involved in the computations. Also all the UEs were considered at fixed position. Hassan *et al.* 2018 mitigated interference using an adaptive network sensing power control technique, which yielded better MUE throughput when compared to node assisted power technique. Their work did not considered co-tier interference, and power consumption of nodes and UE. Also, their technique had complex

means of determining interference. The work of authors in Susanto *et al.* (2017)[a,b], on interference management in downlink and uplink transmission of Femtocell-Macrocell network, presented a simple approach to determining interference in a network which yielded better SINR and also captured both co-tier and cross-tier interference. However, their work did not considered the throughput of UEs and nodes, and the power consumption of nodes and UEs. The power allocation scheme for femto-to-macro downlink interference reduction for smart devices in ambient intelligence, presented by Ali *et al*. (2016) where only co-tier interference was considered. Even thou their power control technique was simple. Authors in Xuan *et al.* (2016), centered on maximizing system throughput in enterprise femtocell network using dynamic power control approach; which yielded a better throughput when benchmark with fixed power control technique. But their work did not captured the effect of co-tier interference, and had a second stage, which will increase memory usage and processing delay, due to more parameters involved. The works of authors in Su *et al.* (2016), considered co-tier and cross-tier interference, their approach gave an average SINR. But they used a complex technique called modified water filing power algorithm for adjusting transmit power. The power control approach in Haining et *al.* (2015), optimized femtocell power. Their research architecture did not considered co-tier interference. While Authors in Sharanya *et al.* (2015) only considered cross-tier interference, though their work when compared with that of dynamic power tuning and HUE power tuning had better femtocell power consumption.

The reviewed works in literatures could not captured in a particular study: co-tier and cross-tier interference, mobile UEs, power consumption of nodes and UEs, and throughput of nodes and UEs. Most of the previous works used complex approach in

determining and adjusting transmit power. The complex mathematical model increase processing time and require more memory for storing various computational variable, which increase the memory requirement of nodes and UEs. This study seeks to address such gaps, by using a simple mathematical model to determine interference in Macro-Femto network. It also seeks to consider both co-tier and cross-tier interference and evaluate the throughput and power usage performance. Table 2.3 presents a summary of the strength and weakness of related and existing power control techniques used for mitigating interference in Macro-Femto HetNet.

Table 2.3: Summary of relevant power control technique for interference mitigation

S/N	Author	Year	Topic	Type of Interference	Strength	Weakness
1	Hassan and Gao	2019	An Active Power Control Technique for Downlink Interference Management in a Two-Tier Macro – Femto Network	Cross –tier only	Good throughput	co-tier interference was not considered, complex and static network
2	Hassan *et al*	2018	Interference Management in Femtocells by the Adaptive Network Sensing Power Control Technique	Cross–tier only	Moderate Macro user throughput	Co-tier interference was not considered
3	Susanto *et al*	2017[b]	Interference Management Using Power Control for Uplink Transmission in Femtocell-Macrocell Network	Co–tier and cross-tier	Good UE SINR when benchmarked	UEs are static and their throughput was not considered.
4	Susanto *et al*	2017[a]	Downlink Power Control for Interference Management in Femtocell-Macrocell Cellular Communication Network	Co–tier and cross-tier	Good base stations SINR	UEs were static and throughput not considered
5	Ali *et al*	2016	An interference mitigation scheme for LTE based femtocell networks	Co–tier only	A simple power control algorithm	Consider only co-tier interference
6	Xuan *et al*	2016	Dynamic Power Control for Maximizing System Throughput in Enterprise Femtocell Networks	Cross-tier	High throughput	Complex and Co-tier interference was not considered
7	Su *et al*	2016	Power Allocation Scheme for Femto-to-Macro Downlink Interference Reduction for Smart Devices in Ambient Intelligence	Co-tier and Cross-tier	Average received SINR	A complex modified water filing (WF) power algorithm was used
8	Haining *et al.*	2015	Femtocell Power Control for Interference Management Based on Macro-Layer Feedback	Cross-tier	Optimized femtocell transmit power	Co-tier interference and uplink transmission was not considered

CHAPTER THREE

3.0 RESEARCH METHODOLOGY

The Enhanced Active Power Control (EAPC) technique is derived from the hybridization of Active Power Control (APC) Technique, Power Control 1 (PC1) technique, and extended attenuation factor model. Step power value of 0.5 dB was used in EAPC. This chapter explains the development of an enhanced power control technique in stages using block diagram and flowchart. It also presents the research Macro-Femto architecture and assumptions in Table 3.1.

Table 3.1: Research assumptions

S/N	Assumptions
1.	UEs are in an obstructed building
2.	All UEs are indoor
3.	Femtocell close access mode
4.	Co-channel deployment
5.	HUE1 is close to en-gNB1
6.	MUE 1 is close to Hen-gNB 2
7.	HUE 2 is close to Hen-gNB 1

3.1 Block Diagram of an Enhanced Active Power Control Technique

The block diagram of an enhanced active power control technique is presented in Figure 3.1 and the various blocks are explained thereafter.

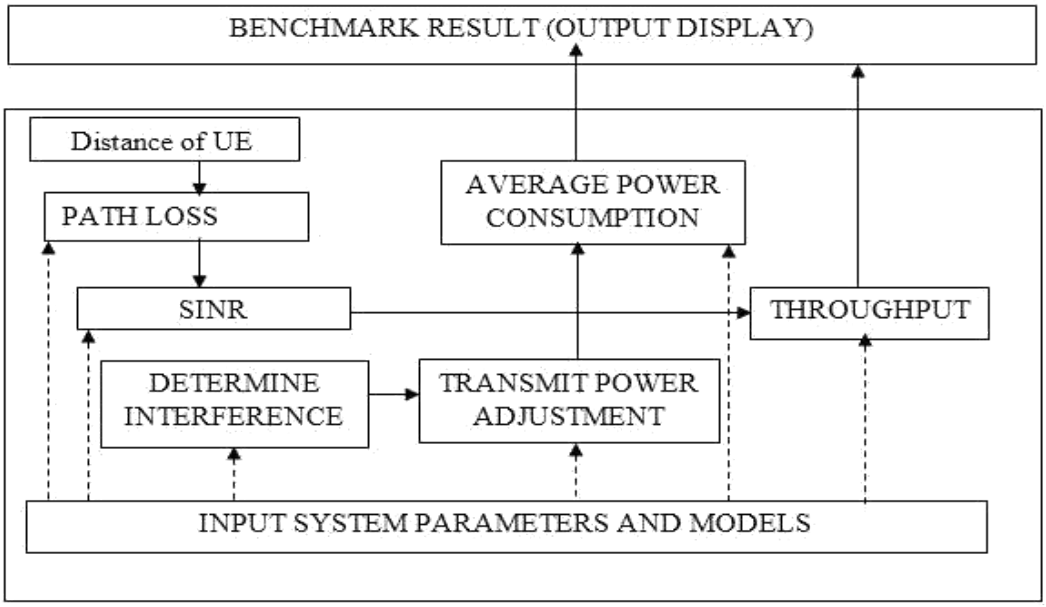

Figure 3.1: A block diagram of enhanced active power control technique

3.1.1 Path loss block

The transmission path loss is computed using mathematical models, system parameters in Table 3.2, and the distance between UEs from their respective nodes. The system parameters were adopted from the anchored papers (Susanto *et al.* 2017[a,b], Hassan and Gao, 2019).

Table 3.2: System parameters of enhanced active power control technique

No.	Parameter	Value
1.	Maximum transmit power of Hen-gNB	20 dBm
2.	Maximum transmit power of en-gNB	46 dBm
3.	Maximum transmit power of HUE and MUE	23 dBm
4.	Minimum transmit power of Hen-gNB, HUE and MUE	0 dBm
5.	Minimum transmit power of en-gNB	5 dBm
6.	Initial transmit power of HUE and MUE	5 dBm
7.	Initial transmit power of Hen-gNB	8dB
8.	Initial transmit power of en-gNB	34 dBm
9.	Thermal noise	-174 dBm
10.	Target SINR	10

(Source: Susanto *et al.* 2017[a,b], Hassan and Gao, 2019)

The path loss between en-gNBs and MUEs is computed using equation (2.14), adopted from Susanto *et al.* (2017) and Hassan and Gao (2019). The femtocell path loss model used to compute propagation loss between Hen-gNBs and HUE is presented in equation (3.4). Equation (3.1), is an extension of attenuation factor model in equation (2.4). It was extended by adding wall attenuation factor ( ).

$$= [\ (\ )]\ + 10\ (\ )+\ + \tag{3.1}$$

where – – stand for path loss when considering femtocell node and its UE, is the distance between femtocell node and UE, [(0)] is free space path loss

given in equation (2.3). Substituting equation (2.3) in equation (3.3) give rise to equation (3.2).

$$= -10\ (\ \frac{\ }{\ }\ )^{2}\ +10\ \frac{\ }{\ }+\ + \tag{3.2}$$

substitute path loss exponent ( ) of 6 (Table 2.1), of 16.2 from Table 2.1 in equation (3.2) to get equation (3.3).

$$= -\log(\ \frac{\ }{4\ *\ 0}\ )^{2}\ +60(\ \frac{\ }{0}\ )+16.2+ \tag{3.3}$$

where stand for wavelength, which is mathematically given in equation (3.4).

$$= \frac{h\ (\ )}{(\ )} \tag{3.4}$$

substituting equation (3.4) in equation (3.3) gives equation (3.5).

$$= -\log(\ \frac{\ }{*4\ *\ 0}\ )^{2}\ +60(\ \frac{\ }{0}\ )+16.2+ \tag{3.5}$$

substituting $= {}^{22}7, = 3 \times 10^{8}\ /$ and $_0 = 1$ and carrier frequency of 2.6 GHz (Rehman *et al.* 2020) in equation (3.5) gives equation (3.6).

$$– \ – \ = 20\log(\ ) + 60\ \ (\ ) - 11.4 + \tag{3.6}$$

where – – is propagation path loss between – and , stands for carrier frequency in MHz, and is the distance between – and . According to Rehman *et al.* (2020), a carrier frequency of 2.6 GHz is used for 5G.

3.1.2 Signal-to-interference-plus-noise-ratio block

At each position of UEs from their serving nodes, the SINR of en-gNB, Hen-gNBs, MUE, and HUEs, is computed using equation (3.9) sourced from Hassan and Gao, 2019, and Susanto *et al*, 2017[b].

$$= \frac{}{} \tag{3.7}$$

where Σ – is total cross-tier interference, Σ – is total co-tier interference

is transmit power of transmitter, – is path loss from transmitter to receiver and is SINR of receiver.

The average SINR of Hen-gNBs, HUEs, en-gNBs, and MUEs considering all the positions of UEs from their nodes is compute using (3.8), (3.9), (3.10), and (3.11) respectively.

$$= \frac{(+ +\cdots+)}{} \tag{3.8}$$

where stand for average SINR of Hen-gNB in the network. Σ = =1 (– 1 + – 2 + ⋯ + –) stand for sum of all Hen-gNB SINR in the network, considering all positions of HUEs, – 1 + – 2 + ⋯ + – stand for sum all Hen-gNB SINR at particular position of HUE, – B is the number of Hen-gNB in the network and

stand for last position of .

$$= \frac{\sum (\quad + \quad + \cdots + \quad)}{} \tag{3.9}$$

where stands for average SINR of HUE in the network, $\sum = (\quad + \quad + \cdots + \quad)$ stand for sum of all HUEs SINR in the network, considering all positions of HUEs, $_1 + \quad _2 + \cdots +$ stand for sum all HUE SINR at particular position of HUE, is the number of HUE in the network andstand for last position of.

$$= \frac{\sum (\quad + \cdots)}{} \tag{3.10}$$

where stand for average SINR of en-gNB, $\sum = (\quad + \quad _2 + \cdots + \quad _)$ stand for sum of all en-gNB SINR in the network, considering all positions of MUEs, $\quad _1 + \quad _2 + \cdots + \quad _$ stand for sum all en-gNB SINR at particular position of HUE, − B is the number of en-gNB in the network and stand for last position of .

$$\Sigma = \frac{(\quad _1 + \quad _2 + \cdots + \quad)}{} \tag{3.11}$$

where stands for average SINR of MUE in the network, $\sum = _{=1} (\quad _1 + \quad _2 + \cdots +)$ stand for sum of all MUEs SINR in the network, considering all positions of MUEs, $_1 + _2 + \cdots +$ stand for sum all MUE SINR at particular position of HUE, is the number of MUE in the network and stand for last position of .

3.1.3 Determine interference block

The Macro-Femto HetNet interference is determined using a simple approach adopted from Susanto *et al*. 2017. Where each nodes and UEs in the network, after measuring it's

received SINR compared it with target SINR to determine interference in the network. The mathematical expression for determining interference in the network is given in equation (3.12).

=– (3.12)

when is greater than , it implies there is approximately no interference and the transmit power is above the minimum power required for communication, hence the power should be reduce. When is less than , it implies that there is interference and the transmit power needed for communication needs to be increased. And when is equal to , the present transmit power will be used for the next transmission.

3.1.4 Power adjustment block

The adjustment of nodes and UEs transmit power is anchored on interference in the Macro-Femto HetNet. The conditions for reducing, maintaining, or even increasing the downlink, uplink transmit power are based on the difference between and . When , adjustment factor (*S*) is assigned a value of -1 and the next transmit power of UEs, Hen-gNB or en-gNB is reduced by EAPC power step value. When = , 0 is assign to *S* and the next transmit power of UEs, Hen-gNB or en-gNB will maintain the present value. And when < , +1 is assigned to *S* and the next transmit power of serving UE, Hen-gNB, or en-gNB is increased by EAPC power step value. The mathematical expressions that show the assignment of value to adjustment factor is given in equation (3.13) and that which gives the adjustment of the next transmit power is given in equation (3.14).

$< 0 \quad = +1 \quad , = \{ > 0 \quad = -1 \quad , = 0 \quad = 0 \quad .$

(3.13)

$= \quad (\quad , \quad ((\quad + \Delta \quad), \quad))$

(3.14)

where, stands for present transmit power of Hen-gNB, Δ stands for EAPC step power value. stands for the minimum transmit power of the transmitter, stands for the maximum transmit power of transmitter, and stands for the next transmit power using EAPC technique for the set time duration (1). After the expiration of 1 the system starts all over again to determine the next transmit power.

3.1.5 Power consumption block

The transmit power used by nodes and UEs at different positions are collated in an array form, and used in calculating the average power consumption of node and UE. The average power used by Hen-gNB in communicating to their respective HUE considering all Hen-gNBs, was computed using equation (3.15).

$$\Sigma \quad (\quad - 1 \quad + \quad - 2 \quad +\cdots+ \quad - \quad) \qquad (3.17)$$

where – is the average transmit power of Hen-gNB. $\sum = 1 (- 1 + - 2 + \cdots + -)$ is the sum of transmit power used by all the Hen-gNBs in communicating to their HUEs at different HUE positions. $- 1 + - 2 +$

$\cdots + -$ stand for sum of transmit power used by all Hen-gNBs in the network at a particular position of HUEs, – stands for the number of Hen-gNBs in the HetNet and stand for last HUE position. The average transmit power of en-gNB considering all positions of MUE is compute using equation (3.16).

$$= \frac{}{(+ \cdots +)} \quad (3.16)$$

where is the average transmit power of en-gNB. $\Sigma = ($ $+$ $_2 + \cdots + _)$ is the sum of transmit power used by all the en-gNBs in communicating to their MUEs at different HUE positions. $_1 + _2 + \cdots +$ $_$ stand for sum of transmit power used by all en-gNBs in the network at a particular MUE position, $_$ stands for the number of en-gNBs in the HetNet, and stand for last MUE position. The average power used by HUE to their serving Hen-gNB is computed using (3.17).

$$\frac{\Sigma^{=} (_1 + _2 + \cdots +)}{} \quad (3.17)$$

where is the average transmit power of HUE. $\Sigma = =1 (_1 + _2 + \cdots +)$ is the sum of transmit power used by all the HUEs at different HUE positions. $_1 + _2 + \cdots +$ stand for sum of transmit power used by all HUEs in the network at a particular HUE position, stand for the number of HUEs in the HetNet, and stand for last HUE position. The average transmit power of MUEs at all positions is compute using equation (3.18).

$$= \frac{}{(+ \cdots +)} \quad (3.18)$$

where is the average transmit power of MUE. $\Sigma = =1 (_1 + _2 + \cdots +)$ is the sum of transmit power used by all the MUEs at different MUE positions. $_1 + _2 + \cdots +$ stand for sum of transmit power used by all MUEs in the network at a particular MUE position, stand for the number of MUEs in the HetNet, and stand for last MUE position.

3.1.6 Throughput block

The throughput of each receiver is computed using equation (3.19) sourced from Hassan and Gao 2019, and 3GPP release. 8.2.

$=\propto 2(1+)$ (3.19) From equation (3.19), the throughput of each HUE, MUE Hen-gNB, and en-gNB are computed using equation (3.20), (3.21), (3.22) and (3.23) respectively.

$$=\propto_2(1+) \quad (3.20)$$

$$=\propto_2(1+) \quad (3.21)$$

$$_{-} =\propto_2(1+ _{-}) \quad (3.22)$$

$$_{-} =\propto_2(1+ _{-}) \quad (3.23)$$

where,, $_{-}$, and $_{-}$ are received SINR by

HUE, MUE, *Hen-gNB* and *en-gNB*, respectively. is channel throughput, $\propto$ is attenuation factor, is system bandwidth, and is SINR of receiver. ,

, $_{-}$ and $_{-}$ are throughput of *HUE*, *MUE*, *Hen-gNB* and *en-gNB*, respectively. System bandwidth of 60 MHZ for 5G network was used, adopted from the work of authors in Rehman *et al.* (2020).

3.2 Research System Architecture and Description

The architecture of the research Macro-Femto HetNet captured both co-tier and cross-tier interference, as illustrated in Figure 3.2. It has one macrocell and two overlaid femtocells.

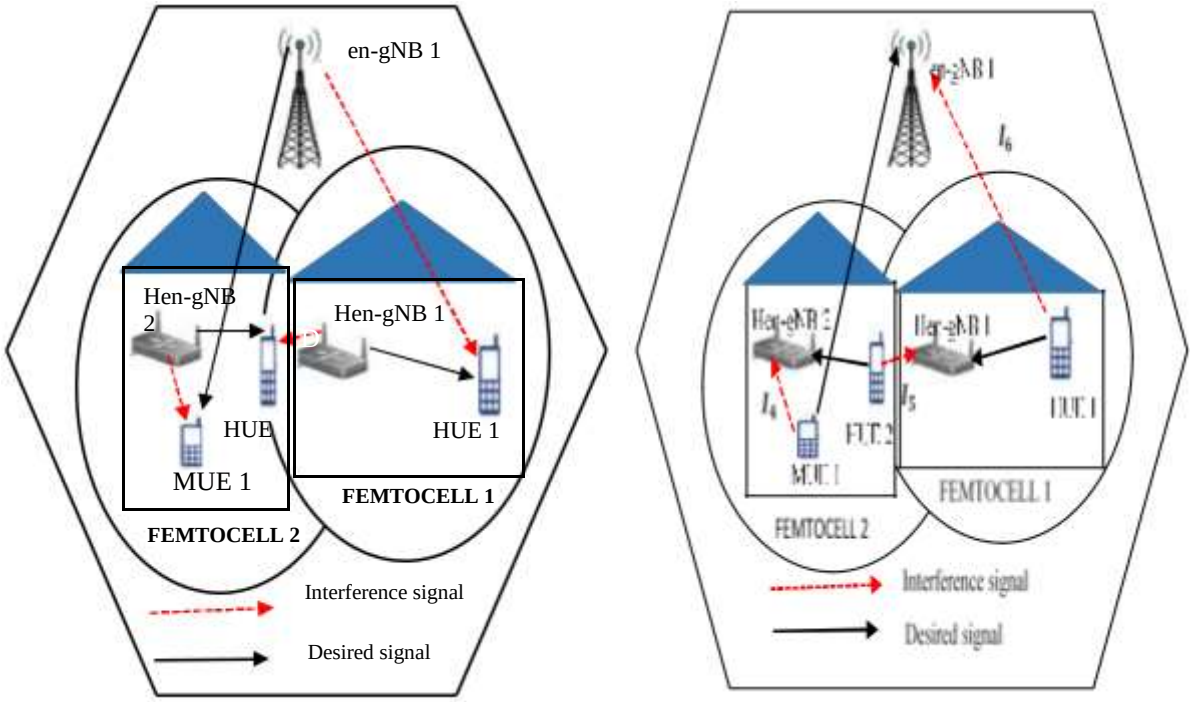

a. Downlink transmission

b. Uplink transmission

Figure 3.2: Research system architecture

From the research architecture in Figure 3.1, $_1$ represents downlink cross-tier interference, where MUE 1 is the VT and Hen-gNB 2 is the AG. $_2$ is a downlink co-tier

interference, in which Hen-gNB 1 is the AG and HUE 2 is the VT. $_3$ is a downlink cross-tier interference, en-gNB 1 is the AG and HUE 1 is the VT. $_4$ is an uplink

cross-tier interference, by which MUE1 is the AG and Hen-gNB 2 is the VT. $_5$ is an uplink co-tier interference whereby HUE 2 is the AG and Hen-gNB 1 is the VT. And $_6$ is an uplink cross-tier interference, in which HUE 1 is the AG and en-gNB 1 is the VT.

3.3 Flowchart of an Enhanced Active Power Control Technique

The flowchart of the an enhanced active power control technique, as presented in Figure 3.3 shows the series of actions and the order in which such actions would be executed to update the uplink transmit power of UEs and downlink power of Hen-gNBs, and en-gNB.

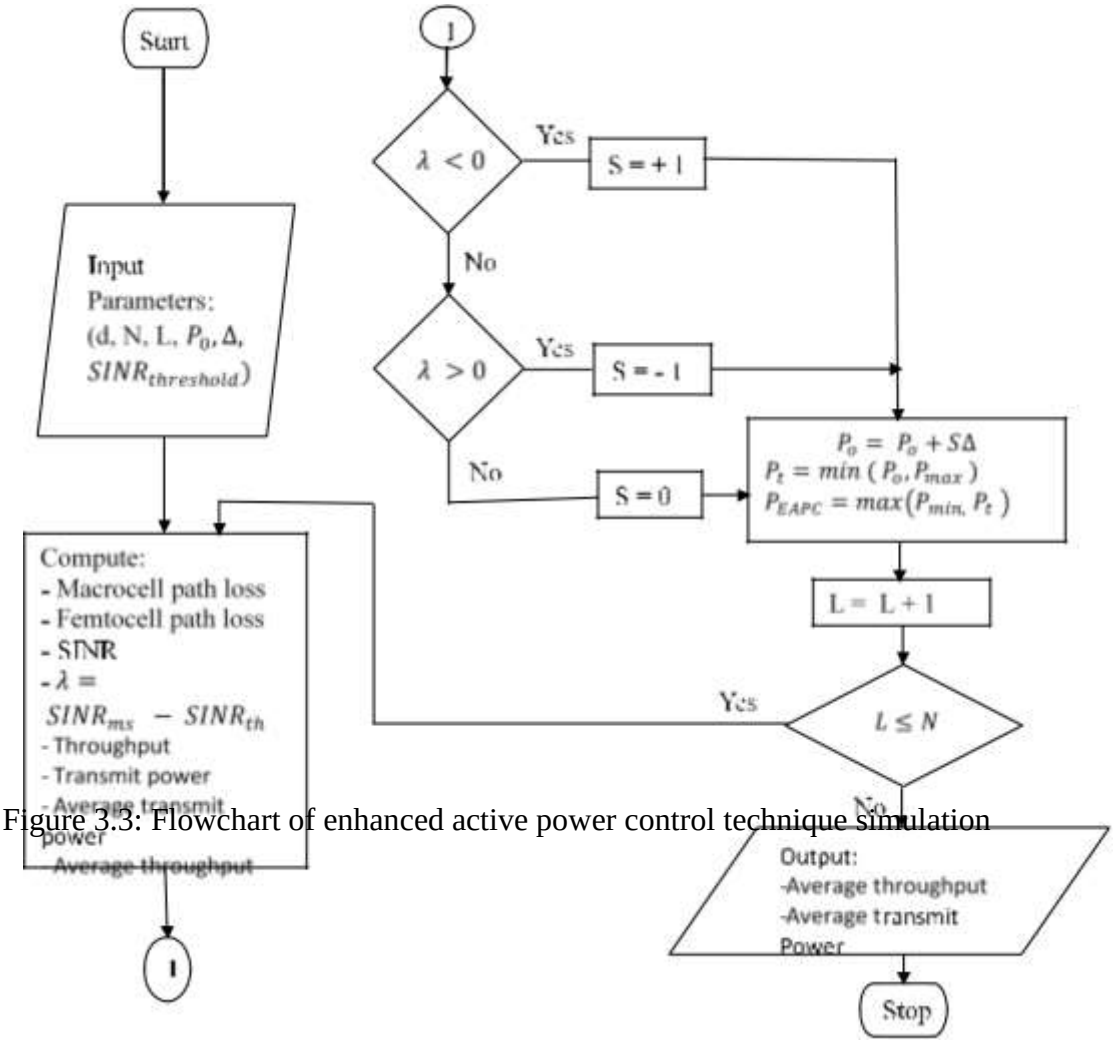

Figure 3.3: Flowchart of enhanced active power control technique simulation

Figure 3.3: Flowchart of enhanced active power control technique simulation

3.4.1 Description of flowchart

When the nodes and UEs boots successfully, the system parameters presented in Table 3.1 are load into their respective memories. The different nodes and UE performed mathematical computation to determine when to adjust or even maintain their transmit power, using mathematical models and specified system parameters. The computations include that of path loss, SINR, the difference between measured and target SINRs, throughput, power adjustment, and average transmit power.

The flowchart of EAPC technique comprises one input stage where system parameters are specified. It has six processes, the first process handles the computation of path loss using equation (3.1) and (3.8) for macrocell and femtocell path loss respectively. The second, third and fourth processes used outcome of computing the difference between measured SINR and target SINR, from the first process to assigned a value to . The fifth process does the actual adjustment of next transmit power within the minimum and maximum transmit power range of nodes and UEs. This is done using the present or initial transmit power, adjustment factor, and EAPC step power value and equation (3.16). The sixth process count the number of iterations. The flowchart has three decision boxes. The first and second decision boxes are used to alter the value assigned to . The third decision box is used to control the number of iterations to be performed.

CHAPTER FOUR

4.0 RESULTS AND DISCUSSION

4.1 Presentation of Results and Discussion

The chapter presents the simulation results of the research Macro-Femto HetNet. The results are broadly categorized into downlink and uplink transmission results. The entire MATLAB codes used for the simulation of the Macro-Femto HetNet are bulky, hence some of the codes that captured all stages of the simulation are presented in appendix A.

The researchers used throughput and energy consumption of UEs and nodes as key performance indicators of the research. This is because of the relationship between interference, throughput and transmit power. Interference in a network is inversely proportional to throughput and directly proportional to transmit power, when other factors are kept constant. That is, the higher the interference the lower the throughput, the higher the throughput the lower the interference. The higher the transmit power the higher the chances of interference, the lower the transmit power the lower the interference. In other words, the higher the transmit power the higher the interference and the lower the throughput. The lower the transmit power the lower the interference and the higher the throughput.

4.2 Downlink Transmission Results

The downlink results obtained from the research simulation includes the throughput of HUE and MUE, and the power consumption of femtocell and macrocell logical node. The average HUE and MUE throughput performance at different position of UEs was computed using equations (3.22) and (3.23), respectively and the result presented in Figures (4.1) and (4.2), respectively. The received SINR was computed using (3.9),

depending on the path loss valued computed using different techniques. When Hen-gNBs transmitted to its HUE at different HUE positions, and en-gNB transmitted to its MUE at different MUE positions. An array of Hen-gNBs and en-gNBs transmit powers was used in computing the average Hen-gNBs and en-gNB transmit power using equations (3.17) and (3.18), respectively; and the results are presented in Figures (4.3) and (4.4) respectively.

4.2.1 Throughput performance of home user equipment

The throughput performance of HUE using APC, EAPC, and PC1 techniques, is presented in Figure 4.1.

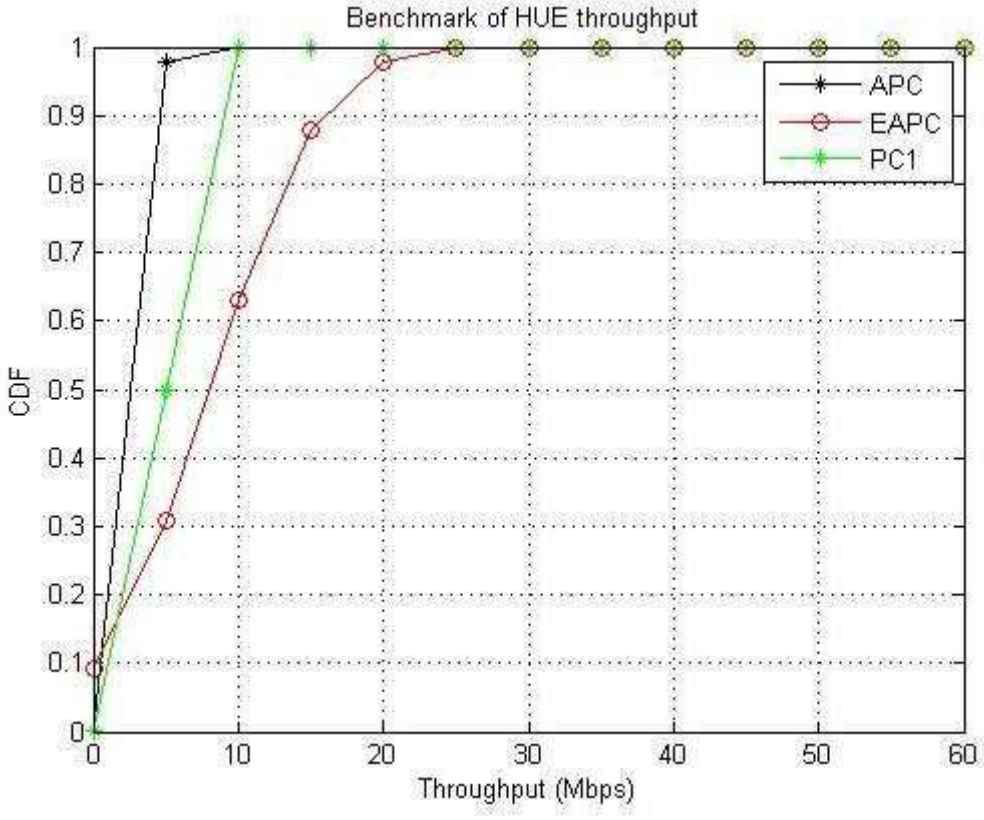

Figure 4.1: Benchmark throughput performance of HUE

In Figure 4.1, at Cumulative Distribution Function (CDF) of 0.2 and above, the EAPC technique had an average HUE that outperformed that of APC and PC1 techniques. Table 4.1 presents the average throughput performance of HUE within the CDF range of 0 – 1.

Table 4.1: Throughput performance of HUE at various CDF values

	HUE Throughput Performance Based on Techniques		
CDF	APC	EAPC	PC1
0.0	0.0	0.0	0.0
0.1	9.0	0.0	1.7
0.2	1.4	2.6	2.2
0.3	1.8	5.2	3.0
0.4	2.3	6.5	4.3
0.5	2.9	8.2	5.2
0.6	3.5	9.6	6.1
0.7	3.9	11.7	7.0
0.8	4.3	13.5	7.8
0.9	4.8	16.1	9.1
1.0	10.0	25.0	10.0

According to Table 4.1, at CDF of 0.1, the HUE throughput of PC1 outperformed that of APC and EAPC techniques by 47% and 100% respectively. At CDF of 0.2, the HUE throughput of EAPC compared to APC and PC1 techniques was higher by 46% and 15%, respectively. At CDF of 0.3, the EAPC HUE throughput compared to APC and PC1 techniques was higher by 65% and 42% respectively. At CDF of 0.4, the EAPC HUE throughput compared to APC and PC1 techniques was higher by 64% and 34% respectively. At CDF of 0.5, EAPC had 65% and 37% higher HUE throughput when compared to APC and PC1 techniques, respectively. At CDF of 0.6, EAPC had 64% and 37% higher HUE throughput when compared to APC and PC1 techniques respectively. At CDF of 0.7, EAPC had 67% and 40% higher HUE throughput when compared to APC and PC1 techniques respectively. At CDF of 0.8, EAPC had 68% and 42% higher HUE throughput when compared to APC and PC1 techniques respectively. At CDF of 0.9, EAPC had 70% and 44% higher HUE throughput when compared to APC and PC1

techniques respectively. At CDF of 1, EAPC had HUE throughput that outperformed that of both APC and PC1 techniques by 60%.

4.2.2 Throughput performance of macro user equipment

The result of comparison between APC, EAPC and PC1 techniques in terms of MUE throughput is presented in Figure 4.2.

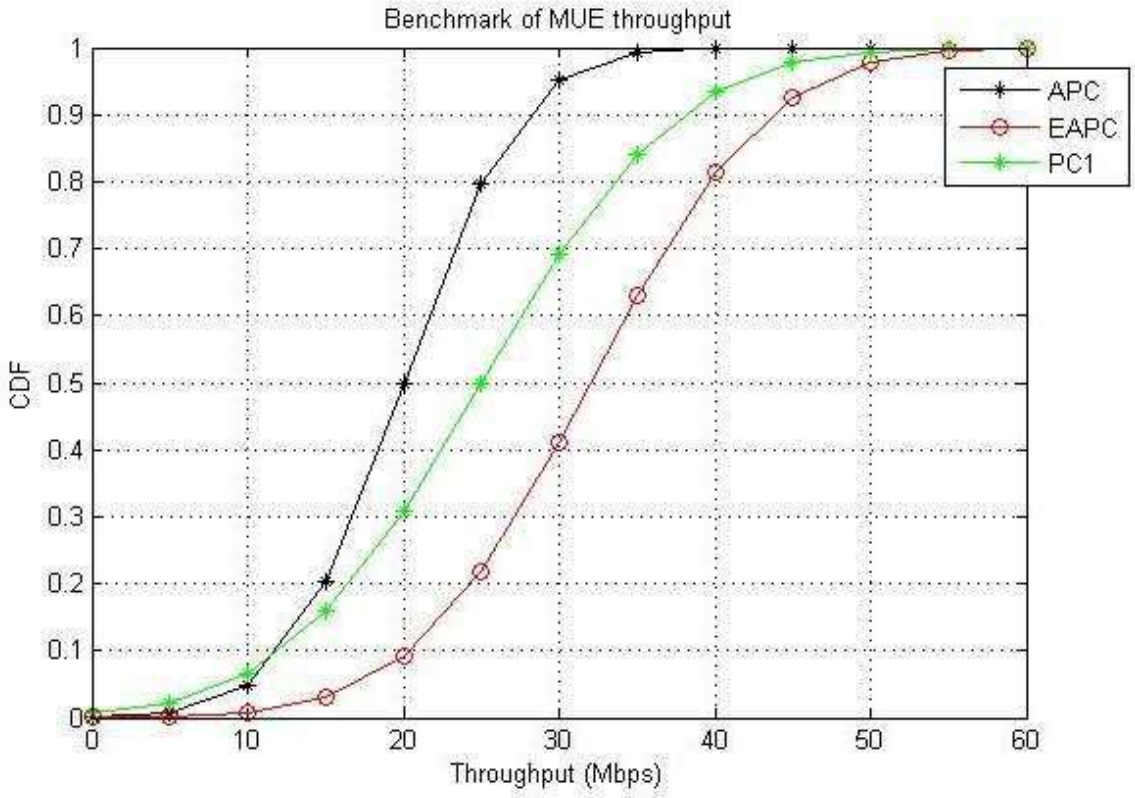

Figure 4.2: Benchmark of MUE throughput

Within the range of 0.1 to 1.0 CDF in Figure 4.2, the MUE throughput, of EAPC technique outperformed that of APC and PC1 techniques. Table 4.2 presents the MUE throughput performances, within the range of 0.1– 1.0 CDF.

Table 4.2: Throughput performance of MUE at various CDF values

	MUE Throughput Performance Based on Techniques in Mbps		
CDF	APC	EAPC	PC1
0	0	0	0
0.1	11.7	20.0	11.7
0.2	15.0	25.0	16.7
0.3	16.7	26.7	20.0
0.4	18.3	29.2	21.7
0.5	20.0	31.7	25.0
0.6	21.7	35.0	26.7
0.7	23.3	36.7	30.0
0.8	25.0	40.0	33.9
0.9	28.3	43.3	38.2
1.0	40.0	55.0	50.0

According to Table 4.2, at 0.1 CDF, the MUE throughput of EAPC outperform that of APC, and PC1 techniques by 42%. At 0.2 CDF, EAPC when compared to APC and PC1 techniques had 40% and 33% higher MUE throughput respectively. At 0.3 CDF, EAPC when compared to APC and PC1 techniques had 38% and 25% higher MUE throughput. At 0.4 CDF, EAPC when compared to APC and PC1 techniques had 37% and 26% higher MUE throughput respectively. At 0.5 CDF, EAPC when compared to APC and PC1 techniques had 37% and 21% higher MUE throughput respectively. At 0.6 CDF, EAPC when compared to APC and PC1 techniques had 38% and 24% higher MUE throughput respectively. At 0.7 CDF, EAPC had 37% and 18% higher MUE throughput when compared to APC and PC1 techniques respectively. At 0.8 CDF, EAPC when compared to APC and PC1 techniques had 38% and 15% higher MUE throughput respectively. At 0.9 CDF, EAPC when compared to APC and PC1 techniques had 35% and 12% higher MUE throughput respectively. At CDF of 1, EAPC when compared to APC and PC1 had 27% and 9% higher MUE throughput techniques respectively.

4.2.3 Transmit power of femtocell node

The benchmark result of the average power used by Hen-gNBs in communicating with their respective HUEs is presented in Figure 4.3.

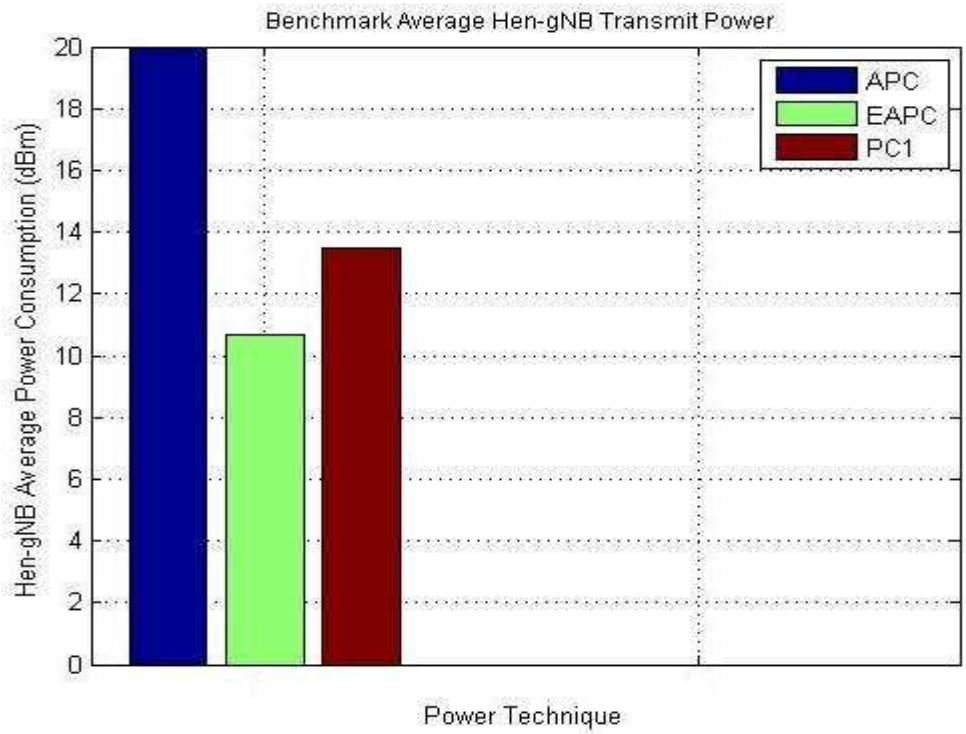

Figure 4.3: Benchmark Hen-gNB power consumption

In Figure 4.3, APC, EAPC, and PC1 techniques had an average Hen-gNB transmit power of 20.00 dBm, 10.65 dBm, and 13.50 dBm respectively. The EAPC technique conserved 47% and 33% Hen-gNB power when compared to APC and PC1 techniques, respectively.

The path loss model used in EAPC gave rise to less signal losses, which improved on received Hen-gNB SINR. When received SINR is above the target SINR, the node will not increase transmit power, rather reduced the transmit power, which accounted for low average Hen-gNB transmit power of EAPC.

4.2.4 Macrocell node power consumption

The benchmark average power consumed by en-gNB in communicating to its MUE is presented in Figure 4.4.

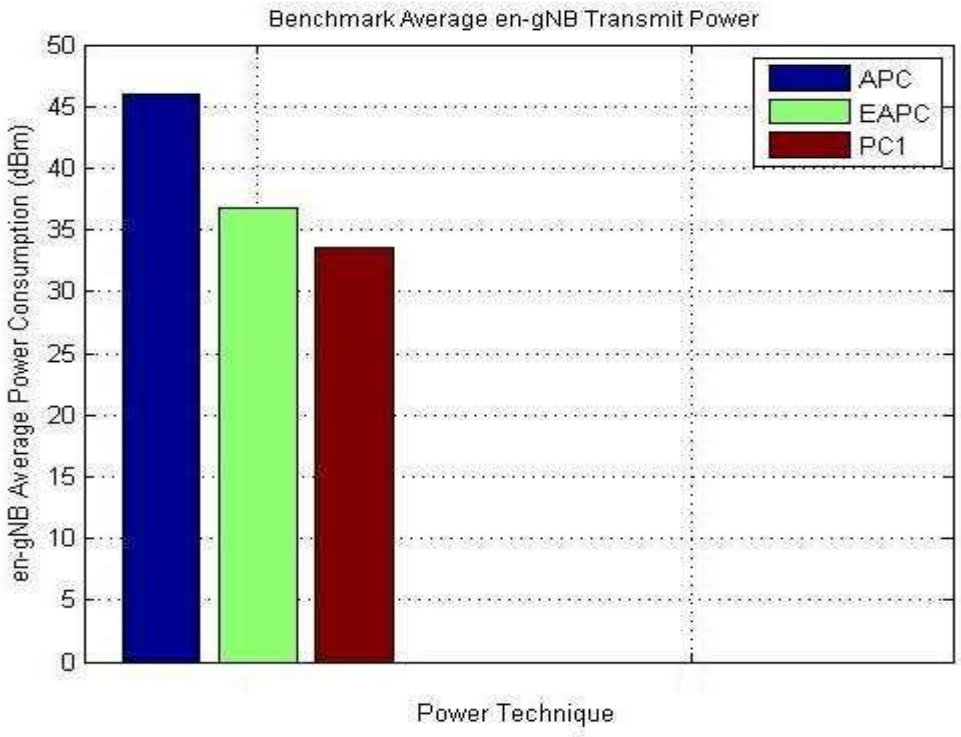

Figure 4.4: Average transmit power of en-gNB

In Figure 4.4, APC, EAPC, and PC1 techniques, had an average en-gNB transmit power of 46.00 dBm, 36.45 dBm, and 33.50 dBm respectively. EAPC technique was limited in conserving en-gNB energy when compare with PC1, while APC technique transmitted at maximum power all through. The EAPC technique conserved 21% of en-gNB power when compared to that of APC technique. While PC1 technique conserved 8% and 27% en-gNB power when compared to EAPC and APC techniques.

4.3 Uplink Transmission Results

The uplink results include the average transmission power of HUE and MUE; and the throughput performance of Hen-gNB and en-gNB. The throughput performance of 51

Hen-gNB and en-gNB was computed using equations (3.24) and (3.25), respectively and the results presented in Figures (4.5) and (4.6), respectively. The array of HUE and MUE transmit powers was used in computing the average transmit power of HUE and MUE using equations (3.19) and (3.20), respectively, and the results presented in Figures (4.7) and (4.8) respectively.

4.3.1 Throughput performance of femtocell node

The comparison of APC, EAPC, and PC1 techniques in regards to throughput performance of Hen-gNB is presented in Figure 4.5.

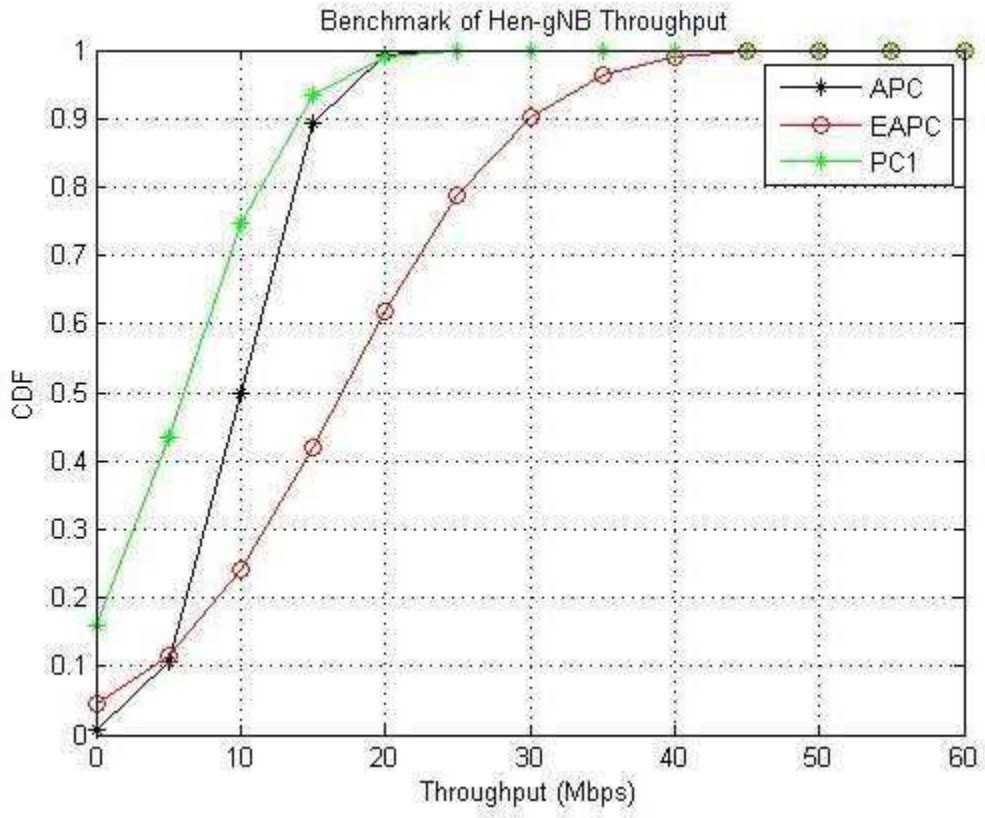

Figure 4.5: Benchmark of Hen-gNB throughput

From Figure 4.5, the Hen-gNB throughput performance of APC, EAPC, and PC1 techniques at different CDF values are presented in Table 4.3.

Table 4.3: Hen-gNB throughputs at various CDF values

	Hen-gNB Throughput Performance Based on Techniques		
CDF	APC	EAPC	PC1
0.0	0.00	0.00	0.00
0.1	05.4	04.6	00.0
0.2	06.2	08.5	01.5
0.3	07.7	12.3	03.1
0.4	08.5	14.6	04.6
0.5	10.0	16.9	06.2
0.6	11.2	19.2	07.7
0.7	13.1	23.1	09.2
0.8	13.8	25.4	12.3
0.9	15.4	30.0	14.6
1.0	20.0	40.0	20.0

From Table 4.3, at CDF of 0.1, APC compared to EAPC and PC1 techniques had 15% and 100% higher Hen-gNB throughput. At CDF of 0.2, EAPC compare to APC and PC1 techniques had 27% and 82% higher Hen-gNB throughput. At CDF of 0.3, EAPC had 37% and 75% higher Hen-gNB throughput when compared to APC and PC1 techniques respectively. At CDF of 0.4, EAPC had 42% and 69% higher Hen-gNB throughput when compared to APC and PC1 techniques. At CDF of 0.5, EAPC had 41% and 63% higher Hen-gNB throughput compare to APC and PC1 techniques respectively. At CDF of 0.6, EAPC had 42% and 60% higher Hen-gNB throughput when compared to APC and PC1 techniques respectively. At CDF of 0.7, EAPC had 43% and 60% higher Hen-gNB throughput when compare to APC and PC1 techniques respectively. At CDF of 0.8, EAPC had 46% and 52% higher HUE throughput when compared to APC and PC1 techniques respectively. At CDF of 0.9, EAPC had 49% and 51% higher throughput than APC and PC1 techniques. At CDF of 1, the Hen-gNB throughput of EAPC outperformed that of both APC and PC1 techniques by 50%. EAPC technique had the best Hen-gNB throughput at CDF values ranging from 0.2 - 1, while APC technique had the best Hen-gNB throughput at CDF value of 0.1.

4.3.2 Throughput performance of macrocell node

The result of en-gNB throughput based on APC, EAPC and PC1 technique is presented in Figure 4.6.

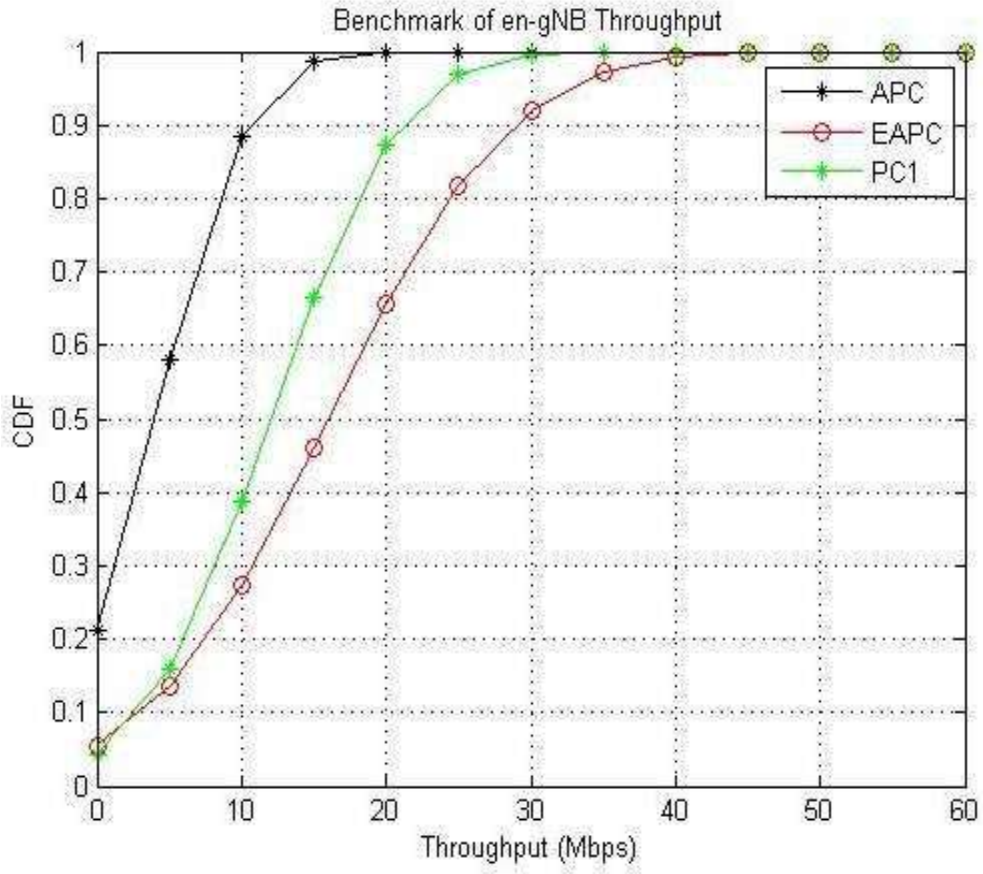

Figure 4.6: Benchmark of en-gNB throughput

From Figure 4.6, the different en–gNB throughput at particular CDF values for APC, EAPC and PC1 techniques are presented in Table 4.3.

Table 4.4: en-gNB throughputs at various CDF values en-gNB Throughput Performance Based on Techniques in Mbps

CDF	APC	EAPC	PC1
0	0.00	0.00	0.00
0.1	0.00	08.0	05.0
0.2	0.00	16.0	11.5
0.3	04.0	22.0	15.0
0.4	06.0	26.0	19.5
0.5	08.0	32.0	23.0
0.6	11.5	36.0	26.0
0.7	13.5	42.5	30.0
0.8	17.0	48.5	34.5
0.9	22.0	56.0	41.0
1.0	40.0	80.0	60.0

According to Table 4.2, at CDF of 0.1, EAPC compare to APC, PC1 and techniques had 100% and 25% higher en-gNB throughput. At CDF of 0.2, EAPC compare to APC and PC1 techniques had 100% and 25% higher en-gNB throughput. At CDF of 0.3, EAPC compare to APC and PC1 techniques had 82% and 23% higher en-gNB throughput. At CDF of 0.4, EAPC compare to APC and PC1 techniques had 78% and 22% higher en-gNB throughput. At CDF of 0.5, EAPC compare to APC and PC1 techniques had 69% and 25% higher en-gNB throughput. At CDF of 0.6, EAPC compare to APC and PC1 techniques had 67% and 22% higher en-gNB throughput. At CDF of 0.7, EAPC compare to APC and PC1 techniques had 65% and 26% higher en-gNB throughput. At CDF of 0.8, EAPC compare to APC and PC1 techniques had 63% and 23% higher en-gNB throughput. At CDF of 0.9, EAPC compare to APC and PC1 techniques had 62% and 26% higher en-gNB throughput. At CDF of 1, EAPC compare to APC and PC1 techniques had 50% and 25% higher en-gNB throughput. EAPC technique had higher en-gNB throughput at CDF of 0.1 – 1.

4.3.3 Transmit power of femtocell user equipment

The average power used for communication between HUE and its respective Hen-gNB in the research Macro-Femto HetNet is presented in Figure 4.7.

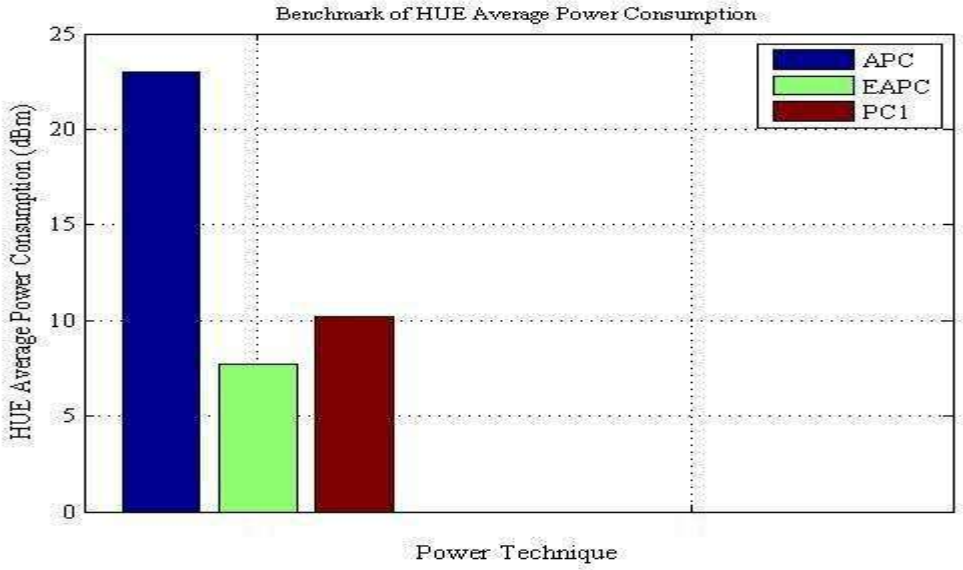

Figure 4.7: Benchmark HUE power consumption

In Figure 4.7 the average transmit power of HUE using EAPC has the lowest power consumption of 7.45 dBm, followed by PC1 with 12.41 dBm, then APC with 21.36 dBm. EAPC technique conserved 65.12 % and 39.97 % of HUE battery when compared with APC and PC1 techniques respectively. The low HUE energy consumption of EAPC technique will increase the battery lifespan of HUE and reduce the probability of having high co-tier and cross-tier interference in the network.

4.3.4 Macrocell user equipment power consumption

The average power used by MUE and en-gNB in communicating at all positions of MUE is presented in Figure 4.8.

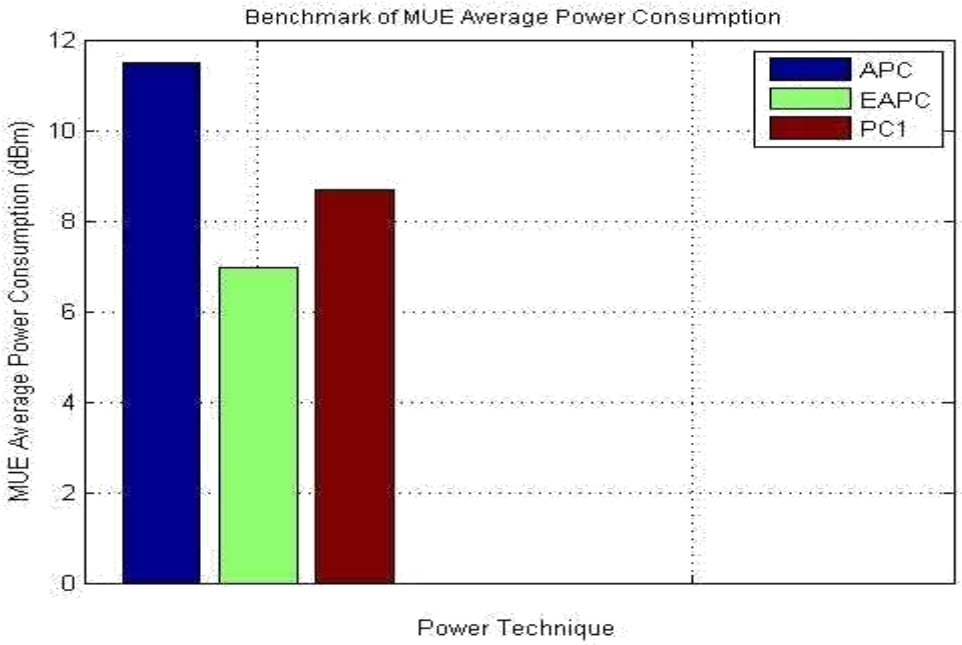

Figure 4.8: Average transmit power of MUE

The MUE transmit power of EAPC had the lowest value of 6.95 dBm, followed by PC1 with 8.70 dBm, and lastly APC with 11.50 dBm. EAPC technique outperformed APC and PC1 in conserving MUE battery by 37.95 % and 42.28 %, respectively.

When interference is reduced, the transmit power of UE also reduced thereby having a less average transmit power. The less interference in uplink transmission of Macro-Femto HetNet when EAPC was used gave less average transmit power of UEs.

CHAPTER FIVE

5.0 CONCLUSION AND RECOMMENDATIONS

5.1 Conclusion

This research work hybridized extended attenuation factor model, power control technique 1, active power control technique, and used a power step value of 0.5 dB to develop an enhanced active power control technique. The research Macro-Femto HetNet architecture considered mobile UEs, two femtocells, one macrocell, two HUEs and one MUE, femtocell close access mode, co-tier and cross-tier interference.

The simulation of the research Macro-Femto HetNet, and comparison of the performance of, the developed EAPC technique with that of APC and PC1 was carried out using MATLAB software, guided by the research assumptions and system parameters. The uplink, downlink Macro-Femto transmission results obtained, as presented in Figures 4.1 – 4.8 indicated that APC technique generally transmitted at high power which accounted for its poor throughput performance, the higher the transmit power the higher the chances of interference and the lower the SINR and throughput. The APC high transmit power is attributed to the second stage power adjustment when mobile UEs were considered. The benchmark results obtained also showed that the EAPC technique that has low interference; as seen in its better throughput and low energy consumption. However the EAPC technique was limited in conserving macrocell node power when compared to that of PC1 technique by. The PC1 technique was better in conserving en-gNB power when compared to EAPC by 8%.

5.2 Recommendations

The developed EAPC technique should be modified to address its limitation of en-gNB power consumptions. As well, the network architecture should be enhanced to capture at least four femtocell nodes, eight home user equipment, and two macro user equipment.

5.3 Contribution to Knowledge

The study developed an enhanced active power control technique for interference mitigation in Macro-Femto cellular network. It also provided a comparative analyses of the performance of EAPC, APC, and PC1 power control techniques, in mobile Macro-Femto HetNet.

REFERENCES

Achonu, A., Caroline, O. A., & Habeeb, B. S. (2020). A New Framework for Interference and Energy Analysis of Soft Frequency Reuse in 5G Networks. *Bulletin of Electrical Engineering and Informatics,* 9(5), 1941 – 1949.

Achonu A., Said, B., & Jeffrey, N. (2017). Interference Modelling for Soft Frequency Reuse in Irregular Heterogeneous Cellular Networks. *International Conference on Ubiquitous and Future Networks (ICUFN),* 9, 381 -386.

Adeyemo, O., Dlodlo, M., & Ohize, H. (2015). Mitigating Cross-Tier Cross-Boundary Interference in Fractional Frequency Reuse Scheme for Multi-Tier Networks. In *AFRICON* (IEEE), 1 - 6.

Agiwal, M., Roy, A. & Saxena, N. (2016). Next Generation 5G Wireless Networks: A Comprehensive Survey. *IEEE Communications Surveys and Tutorials.* (18)3, 1617 - 1655.

Ali, S. G., Baba, D. M., Zan, M. M., Rahman, R. A., Saif, A., Yusof, M. I, & Azmat, F. H. (2016). An Interference Mitigation Scheme for LTE Based Femtocell Networks. *AIP Conference Proceeding,* 7(1), 5002 -5062.

Amandeep, Sanjeev, K., Vikas, C., & Prem, K. (2019). LTE-A Heterogeneous Networks UsingFemtocells. *International Journal of Innovative Technology and Exploring Engineering (IJITEE),* 8(4), 2278 – 3075.

Afolalu, O. F., Petinrin, J. O., & Ayoade, M. A. (2016). A Survey of Interference Challenges and Mitigation Techniques in 5G Heterogeneous Cellular Networks. *International Conference of Sciences, Engineering & Environmental Technology (ICONSEET),* 1(2), 8 - 14.

Al-omari, M., Ramli, A. R., Sali, A. & Azmir, R. S. (2016). A Femtocell Cross-Tier Interference Mitigation Technique in OFDMA-LTE System: A Cuckoo Search Based Approach. *Indian Journal of Science and Technology,* 9(17), 899-896.

Andrian, D. A., Wayan, M., & Sigit, B. W. (2015). Downlink Cross-Tier Interference Mitigation for Macrocell User in Open Access Femtocell Using Handover Scenario. *International Conference on Electrical Engineering and Informatics,* 5, 656 – 660.

Aneeqa, I., Syed, A. H., & Dushantha, N. (2017). A Multiple Region Reverse Frequency Allocation Scheme for Downlink Throughput Enhancement in 5G HetNets. *IEEE Annual Consumer Communications & Networking Conference (CCNC),* 14, 905 – 910.

Asif, M. H., Nasimi, M., Han, B., & Schotten, H. D. (2019). A Comprehensive Survey of RAN Architectures Toward 5G Mobile Communication System. *IEEE Access,* 7, 70371 – 70421.

Dawar, K. P., Usman, A.U, & Salihu, B. A. (2021). An Enhanced Active Power Control

Technique for Interference Mitigation in 5G Uplink Macro-Femto Cellular Network. *IEEE International Conference on Cyberspace (CYBER NIGERIA),* 2, 85-90.

Farah, R., Asif, R., & Khaizuran, A. (2016). Advanced Inter-Cell Interference Management Technologies in 5G Wireless Heterogeneous Networks (HetNets). *IEEE Student Conference on Research and Development (SCOReD)*, 1 - 4.

Feng, M., Li, G., & Gong, W. (2018). Heterogeneous Network Resource Allocation Optimization Based on Improved Bat Algorithm. *International Conference on Sensor Networks and Signal Processing (SNSP),* 55 -59.

Gurpreet, S., Rahul, M., & Abdesh, S., (2016). Femtocell: History, Technical Issues and Challenges. *International Research Journal of Engineering and Technology (IRJET)*, s 03(5), 93 – 105.

Haroon, M. S., Abbas, Z. H. Muhammad, & F. Abbas, G. (2019). Coverage Analysis of Cell-Edge Users in Heterogeneous Wireless Networks Using Stienen's Model and RFA Scheme. *International Journal of Communication,* 1 – 17.

Hassan, T. U., & Gao, F. (2019). An Active Power Control Technique for Downlink Interference Management in a Two-Tier Macro–Femto Network. *Journal of Sensors*, 19(9), 504 - 528.

Hassan, T. U., Gao, F., Jalal, B., & Arif, S. (2018). Interference Management in Femtocells by the Adaptive Network Sensing Power Control Technique. *Journal of Future Internet*, 10(3), 2015 -2028.

Haining, W. Chenxi, Z., & Zhi, D. (2015). Femtocell Power Control for Interference Management Based on Macro-Layer Feedback. *IEEE transaction on Vehicular Technology.*

Heli, Z., Shanzhi, C., Xi, L., Hong, J., & Xiaojiang, D. (2015). Interference Management for Heterogeneous Networks with Spectral Efficiency Improvement. *IEEE Wireless Communications,* 22(2), 101 – 107.

Imane, Z., Mazri, T. & Amine, E. (2020). 5G: Architecture Overview and Deployments Scenarios. *International Conference on Smart City Application,* 5, 435 – 440.

Jundhare, M. D., & Kulkarni, A. V. (2016). An Overview and Current Development of Femtocells in 5G Technology. *IEEE International Conference on Advances in Electronics, Communication and Computer Technology (ICAECCT)*, 204 - 209.

Jinlong, W., Long, W., Qihui, W., Panlong, Y., Yuhua, X., & Jing, W. (2015). Less Is More: Creating Spectrum Reuse Opportunities via Power Control for OFDMA Femtocell Networks. *IEEE Systems Journal,* 10(4), 1470 – 1481.

Meer Z. N., & Kaleem, U. M. (2020). A Review Of 5G Technology: Architecture, Security and wide Applications. *International Research Journal of Engineering and Technology (IRJET)*, 7(5), 1-35.

Mohammad, G., Gobi, V., Elias, G., & Soheil, M. M. (2019). Capacity Improvement in 5G Networks Using Femtocell. *Wireless Personal Communications,* 105(3), 1027 – 1038.

Mythili, A. & Mahendran, S. K. (2017). A Study of 5G Network: Structural Design, Challenges and Promising Technologies, Cloud Technologies. *International Journal of Advanced Research, Ideas and Innovations in Technology,* 3(6), 325 – 339.

Onu, C., Bala. S. A., & Abolarinwa J. (2018). Enhanced Fractional Frequency Reuse in LTE A Heterogeneous OFDMA Network. *ATBU, Journal of Science, Technology & Education (JOSTE),* 6 (2), 18 – 27.

Priya, T., & Seema, H. (2017). Cognitive Femtocell Network Various Challenges and Security Issues. *International Conference on Computing Methodologies and Communication (ICCMC),* 1 – 5.

Rappaport T. S. (2002). *Wireless Communication Principles and Practice,* (2nd ed.). New Jersey: Prentice hall PTR.

Rehman, S. U., Hussain, A., Hussain, F., & Mannan, M.A. (2020). A Comprehensive Study: 5G Wireless Networks and Emerging Technologies. *International Electrical Engineering Conference (IEEC 2020),* 5, 25-32.

Sajjad, A. K., Muhammad, A., Kerem, K., & Adnan, K. (2018). A Power Control Algorithm and Software Tool for Femtocells in LTE-A Network. *Sakarya University Journal of Science,* 22(4), 1124-1129.

Sharanya, R., Gunasundari, R., & Jayanthi, K. (2015). Dynamic Power Tuning For Downlink Interference Mitigation in Heterogeneous LTE Network. *ARPN Journal of Engineering and Applied Science*, 10, 1810 - 1814.

Su, X., Liang, C., Choi, D., & Choi, C. (2016). Power Allocation Scheme for Femto-to-Macro Downlink Interference Reduction for Smart Devices in Ambient Intelligence. *Mobile Information Systems.* 5(2), 16-20.

Susanto, M., Fauzia, D. & Alam, S. (2017)[a]. Downlink Power Control for Interference Management in Femtocell-Macrocell Cellular Communication Network. *International Conference on Quality in Research (QiR): International Symposium on Electrical and Computer Engineering*, 15, 479 - 484.

Susanto, M., Hutabarat, R., Yuniati, Y., & Alam, S. (2017)[b]. Interference Management using Power Control for Uplink Transmission in Femtocell-Macrocell Cellular Communication Network. *International Conference on Quality in Research (QiR): International Symposium on Electrical and Computer Engineering*, 15, 245 - 250.

Syed, A. U. & Aashish, P. (2017). Maximization of SINR in Femtocell Network. *International Journal of Electrical, Electronics and Computer Engineering* 6(1), 114 – 117.

Tarte, P., & Hanchate, S. (2017). Cognitive Femtocell Network: Various Challenges and Security Issues. *International Conference on Computing Methodologies and Communication (ICCMC)*, 1 - 5.

Third Generation Partnership Project (3GPP) TR 36.942 version 8.2.0 Release 8. (July, 2009). LTE; Evolved Universal Terrestrial Radio Access (E-UTRA); Radio Frequency (RF) System Scenarios.

Third Generation Partnership Project (3GPP) TR 21.915 Version 15.0.0. (October, 2019). Digital Cellular Telecommunication System; Universal Mobile Telecommunication System (UMTS); LTE; 5G.

Tuan, L., Nguyen, H.T., Sungwon, L., Eui-Nam, H., Zhu, H., & Choong, S.H. (2017). Distributed Power and Channel Allocation for Cognitive Femtocell Network Using a Coalitional Game in Partition-Form Approach. *IEEE Transactions on Vehicular Technology*, 66(4), 3475 – 3490.

Xu, W., & Qiu, R. (2018). Power Allocation for Uplink Cognitive Heterogeneous Network with Non-Orthogonal Multiple Access. *IEEE International Conference on Computer and Communications (ICCC)*, 4, 668 - 672.

Xuan, Z., Gang, W., Gang, F., Shuang, Q., & Yantao, G. (2016). Dynamic Power Control for Maximizing System Throughput in Enterprise Femtocell Networks. *International Conference on Networking and Network Applications*, 184 – 189.

APPENDIX A (Some Macro-Femto Mobile Network Simulation Codes)

```
clc; clear all; close all;
% PROGRAM TO COMPUTE AND COMPARE PC 1, APC AND EAPC MODEL
NETWORK CAPACITY
HeNB_Min_P = 0;% min transmit power of HeNB
HeNB_Max_P= 20;% max transmit power of HeNB
eNB_Min_P = 5;% min transmit power of eNB
eNB_Max_P= 46; % max transmit power of eNB
APC_P_HeNB = HeNB_Initial_Power= 8; APC_P_eNB
= eNB_Initial_Power;
EAPC_P_eNB = eNB_Initial_Power =
34; EAPC_P_HeNB =
HeNB_Initial_Power; PC1_P_eNB =
eNB_Initial_Power; PC1_P_HeNB =
HeNB_Initial_Power; HeNB_RSTP = 20;
eNB_RSTP = 46;
HUE_Min_P = MUE_Min_P = 0;       % min transmit power of HUE
HUE_Max_P= MUE_Max_ P= 23;      % max transmit power of HUE
MUE_initial_P = 5;
HUE_initial_P = 5;
PC1_P_MUE = MUE_initial_P;
PC1_P_HUE = HUE_initial_P;
APC_P_MUE = MUE_initial_P;
APC_P_HUE = HUE_initial_P;
EAPC_P_MUE = MUE_initial_P;
EAPC_P_HUE = HUE_initial_P;
MUE_RSTP = 23;
HUE_RSTP = 23;
Number_of_eNB = 1;  % number of eNB
Number_of_MUE = 1; % number of MUE
Number_of_HeNB = 2;  % number of HeNB
Number_of_HUE = 2; % NUMBER OF HUE
APC_Log_N_Sha_Macro = 8;    % APC eNB LOG SHADOWING STANDARD DEVIATION
APC_Log_N_ Sha = 4; % APC HeNB LOG SHADOWING STANDARD
DEVIATION
APC_INT_THRESHOLD = -72;
APC_L1 = 20;
EAPC_L1 = 10;
PC1_L1 = 10;
FAF = 16.2; % FLOOR ATTENUATION FACTOR
f = 2600; % carrier frequency in MHz
R = 4900;   % distance between eNB and indoor MUEs (DESIRED)
R1 =1000;   % DISTANCE BETWEEN eNB AGGRESSOR AND indoor HUE
R2 = 10;    % distanc between HeNB and indoor UEs (DESIRED)
R3 = 5;    % DISTANCE BETWEEN HeNB AGGRESSOR AND indoor UE VICTIM
R4 = 10;    % DISTANCE B/W HeNB2 AND MUE (UNDESIRED CROSS-TIER)
N = -174;    % value of thermal noise
BW = 60;     % MHz
lf =0.05;           %
SINR_target = 10;
EAPC_MACRO_THROUGHPUT_ARRAY = cell(1,10);
EAPC_FEMTO_THROUGHPUT_ARRAY = cell(1,10);
EAPC_HeNB_P_ARRAY = cell(1,10);
EAPC_eNB_P_ARRAY = cell(1,10);
EAPC_MUE_SINR_ARRAY= cell(1,10);
EAPC_HUE_SINR_ARRAY= cell(1,10);
EAPC_MUE_THROUGHPUT_ARRAY = cell(1,10);
EAPC_HUE1_THROUGHPUT_ARRAY= cell(1,10);
EAPC_HUE2_THROUGHPUT_ARRAY= cell(1,10);
EAPC_MUE_HUE_THROUGHPUT_ARRAY = cell(1,10);
```

```
UPLINK_EAPC_MACRO_ARRAY = cell(1,10);
UPLINK_EAPC_FEMTO_ARRAY = cell(1,10);
EAPC_HUE_P_ARRAY = cell(1,10);
EAPC_MUE_P_ARRAY = cell(1,10);
EAPC_eNB_SINR_ARRAY = cell(1,10);
EAPC_HeNB_SINR_ARRAY = cell(1,10);
EAPC_eNB_THROUGHPUT_ARRAY= cell(1,10);
EAPC_HeNB1_THROUGHPUT_ARRAY= cell(1,10);
EAPC_HeNB2_THROUGHPUT_ARRAY= cell(1,10);
UPLINK_EAPC _FM_ARRAY = cell(1,10);
spv = 0.5;
Number_of_loop = 10;
for x = 1:Number_of_loop, % BEGINNING OF LOOP
R = R +10 ; % distance between eNB and indoor MUEs (DESIRED)
R1 =R1 +10; % DISTANCE BETWEEN eNB AGGRESSOR AND indoor HUE
VICTIM(UNDESIRED CROSS-TIER)
R2 =R2+ 2;    % distanc between HeNB and indoor UEs (DESIRED)
R3 =R3 +2;    % DISTANCE BETWEEN HeNB AGGRESSOR AND indoor UE VICTIM
R4 =R4 +1; % DISTANCE B/W HeNB2 AND MUE (UNDESIRED CROSS-TIER) %
path loss of en-gNB to indoor MUE based on APC model
    APC_ PL_eNB_indoor_MUEs_dB= 10*log10(37.6*log10(R) + 15.3)
+ APC_L1;
 % path loss of en-gNB to indoor MUE based on EAPC model
    EAPC_ PL_eNB_indoor_MUEs_dB = 10*log10(37.6*log10(R) + 15.3) +
EAPC_L1;
 % PATH LOSS OF en-gNB TO INDOOR MUEs using PC1 Model
    PC1_PL_eNB_indoor_MUEs_dB = 10*log10(37.6*log10(R) + 15.3) +
PC1_L1;
% path loss from Hen-gNB to INdoor DESIRED HUE using APC
    APC_PL_HeNB_to_indoor_HUE_dB = 10*log10(log10(R2)*20 + 38.46);
% path loss from Hen-gNB to INdoor HUE using EAPC
   EAPC_PL_HeNB_to_indoor_HUE_dB = 20*log10((4*3.142*f)/(3*10^8)) +
60*log10(R2)+ FAF ;
 % path loss from Hen-gNB - DESIRED indoor HUEs using PC1 model
    PC1_PL_HeNB_indoor_HUE_dB = 10*log10(30*log10(R2/1000) + 127);
 % path loss from Hen-gNB AGGRESSOR to INdoor HUE VICTIM using APC:CO-
TIER
    APC_INT_PL_HeNB_to_indoor_HUE_dB = 10*log10(log10(R3)*20
+ 38.46)+APC_L1;
% path loss from Hen-gNB AGGRESSOR to INdoor HUE VICTIM using EAPC:
CO - TIER
    EAPC_INT_PL_HeNB_to_ indoor_HUE_dB =
20*log10((4*3.142*f)/(3*10^8)) + 60*log10(R3)+ FAF ;
% path loss from Hen-gNB AGGRESSOR - indoor HUEs VICTIM using
PC1 model: CO TIER
    PC1_INT_PL_HeNB_indoor_HUE_dB = 10*log10(30*log10(R3/1000) +
127)+PC1_L1;
% path loss from Hen-gNB AGGRESSOR to INdoor MUE VICTIM using
APC:CROSS TIER
    APC_INT_PL_HeNB_to_indoor _MUE_dB = 10*log10(20*log10(R4) + 38.46);
% INTERFERENCE PATH LOSS
 % path loss from Hen-gNB AGGRESSOR to INdoor MUE VICTIM using EAPC:
CROSS TIER
    EAPC_INT_PL_HeNB_to _indoor_MUE_dB =
20*log10((4*3.142*f)/(3*10^8)) + 60*log10(R4)+ FAF ;
% path loss from Hen-gNB AGGRESSOR - indoor MUEs VICTIM using
PC1 model: CROSS TIER
    PC1_INT_PL_HeNB_indoor_MUE_dB = 10*log10(30*log10(R4/1000) + 127);
% path loss of en-gNB AGGRESSOR to indoor HUE VICTIM USING APC
MODEL: CROSS
% TIER interference scenario
```

```
    APC_INT_PL_eNB_indoor_HUEs_dB = 10*log10(37.6*log10(R1) +
15.3)+ APC_L1; % INTERFERENCE PATH LOSS
 % path loss of en -gNB AGGRESSOR to INdoor HUE VICTIM USING
EAPC MODEL: CROSS TIER
    EAPC_INT_PL_ eNB_indoor_HUEs_dB = 10*log10(37.6*log10(R1)
+ 15.3)+EAPC_L1;
 % PATH LOSS OF en-gNB Aggressor TO INDOOR HUEs using PC1 Model:
CROSS TIER
    PC1_INT_PL_eNB_indoor_HUEs_dB = 10*log10(37.6*log10(R1) + 15.3) +
PC1_L1; % INTERFERENCE PATH LOSS
% SINR OF HUE1 BASED ON EAPC APPROACH
    EAPC_SINR_HUE1  =
EAPC_P_HeNB1*EAPC_PL_HeNB_to_indoor_HUE_dB/((EAPC_P_eNB*EAPC_INT_PL_eN
B_indoor_HUEs_dB) + N);

% SINR OF HUE2 BASED ON EAPC
    APPROACH EAPC_SINR_HUE2 =
EAPC_P_HeNB2*EAPC_PL_HeNB_to_indoor_HUE_dB/((EAPC_P_HeNB1*EAPC_INT_PL
_ HeNB_to_indoor_HUE_dB) + N);

% SINR OF MUE BASED ON EAPC
    APPROACH EAPC_SINR_MUE =
EAPC_P_eNB*EAPC_PL_eNB_indoor_MUEs_dB/(EAPC_P_HeNB2*EAPC_INT_PL_HeNB_
t o_indoor_MUE_dB + N);

%PROGRAM TO COMPUTE EAPC AND PC1 POWER ALPOSITION
  EAPC_HUE1_SINR_DIFF = EAPC_SINR_HUE1 - SINR_target;
  EAPC_HUE2_SINR_DIFF = EAPC_SINR_HUE2 - SINR_target;
  EAPC_eNB_MUE_SINR_DIFF = EAPC_SINR_MUE - SINR_target;

%PROGRAM TO COMPUTE eNB POWER ALPOSITION
  % EAPC power control codes if
 EAPC_eNB_MUE_SINR_DIFF > 0
     EAPC_eNB_c1 = -1;
    elseif EAPC_eNB_MUE_SINR_DIFF <
             0 EAPC_eNB_c1 = 1;
    else EAPC_eNB_c1
      = 0;
 end
  % EAPC power control codes if
    EAPC_HUE1_SINR_DIFF > 0
            EAPC_c2 = -1;
    elseif EAPC_HUE1_SINR_DIFF <
              0 EAPC_c2 = 1;
    else
        EAPC_ c2=0;
    end
    if EAPC_HUE2_SINR_DIFF >
            0 EAPC_c22 = -1;
    elseif EAPC_HUE2_SINR_DIFF <
              0 EAPC_c22 = 1;
    else
        EAPC_c22=0
        ; end

  % COMPUTE POWER ADJUSTMENT OF HeNB TRANSMIT POWER
   EAPC_P_HeNB1 = min(max(HeNB_Min_P,(EAPC_P_HeNB1 +
(EAPC_c2*spv))),HeNB_Max_P);% to ensure that transmit power (P_2) is
between EAPC_P_HeNB2 = min(max(HeNB_Min_P,(EAPC_P_HeNB2 +
(EAPC_c22*spv))),HeNB_Max_P);% to ensure that transmit power (P_2) is
between
```

```
% COMPUTE power ADGUSTMENT OF eNB transmit power
  EAPC_P_eNB = max(min(eNB_Max_P,(EAPC_P_eNB +
(EAPC_eNB_c1*spv))),eNB_Min_P); % to ensure that transmit power
(P_3) is
 % MUE SINR ARRAY
     EAPC_MUE_SINR_ARRAY{x}= EAPC_SINR_MUE ;
 % HUE AVERAGE SINR ARRAY
     EAPC_HUE_SINR_ARRAY{x}=
(EAPC_SINR_HUE1+EAPC_SINR_HUE2)/Number _of_HUE ;
% COMPUTE CAPACITY OF EACH UE (MUE, )
    EAPC_Capacity_MUE = lf*BW*log2(1 + EAPC_SINR_MUE);
% COMPUTE CAPACITY OF MACROCELL AND FEMTOCELL
    EAPC_Avg_Capacity_Macro = EAPC_Capacity_MUE/ Number_of_MUE ;
    EAPC_MACRO_THROUGHPUT _ARRAY{x}= EAPC_Avg_Capacity_Macro ;
% CAPACITY BASED ON EAPC
    EAPC_Capacity_HUE1  =  lf*BW*log2(1  +  EAPC_SINR_HUE1);
    EAPC_Capacity_HUE2 = lf*BW*log2(1 + EAPC_SINR_HUE2);
% COMPUTE CAPACITY OF MACROCELL AND FEMTOCELL
EAPC_MUE_THROUGHPUT_ARRAY{x}=EAPC_Capacity_MUE
EAPC_HUE1_THROUGHPUT_ARRAY{x}=EAPC_Capacity_HUE1;
EAPC_HUE2_THROUGHPUT_ARRAY{x}=EAPC_Capacity_HUE2;
EAPC_MUE_HUE_THROUGHPUT_ARRAY{x}=EAPC_Capacity_MUE
+ EAPC_Capacity_HUE1 +EAPC_Capacity_HUE2;
% computation of Avg cpacity of femto and macro network
(sum/no) EAPC_Avg_Capacity_Femto = (EAPC_Capacity_HUE1
+EAPC_Capacity_HUE2)/Number_of_HUE ;

EAPC_FEMTO_THROUGHPUT_ARRAY{x}= EAPC_Avg_Capacity_Femto
; %HeNB Average power consumption
   EAPC_HeNB_P_ARRAY{x} =(EAPC_P_HeNB1 +EAPC_P_HeNB2)/Number_of_HeNB
; %eNB power consumption
    EAPC_eNB_P_ARRAY{x} = EAPC_P_eNB;

  % COMPUTE UPLINK SINR OF HeNB1 BASED ON EAPC MODEL
    UPLINK_EAPC_SINR_HeNB1 =
EAPC_P_HUE1*EAPC_PL_HeNB_to_indoor_HUE_dB/((EAPC_P_HUE2*EAPC_INT_PL_H
e NB_to_indoor_HUE_dB) + N)

% UPLINK SINR OF HeNB2 BASED ON EAPC
    MODEL UPLINK_EAPC_SINR_HeNB2 =
EAPC_P_HUE2*EAPC_PL_HeNB_to_indoor_HUE_dB/((EAPC_P_MUE*APC_INT_PL_HeN
B _to_indoor_MUE_dB) + N);

% UPLINK SINR OF eNB BASED ON EAPC
APPROACH UPLINK_EAPC_SINR_eNB =
EAPC_P_MUE*EAPC_PL_eNB_indoor_MUEs_dB/((EAPC_P_HUE1*EAPC_INT_PL_eNB_i
n door_HUEs_dB) + N);
  end
%PROGRAM TO COMPUTE EAPC AND PC1 UPLINK (MUE) POWER ALPOSITION
    SINR_eNB_DIFF_EAPC = UPLINK_EAPC_SINR_eNB - SINR_target;

% PROGRAM TO COMPUTE EAPC AND PC1 HUE UPLINK POWER ALPOSITION
    SINR_HeNB1_DIFF_EAPC  =  UPLINK_EAPC_SINR_HeNB1  -  SINR_target;
    SINR_HeNB2_DIFF_EAPC = UPLINK_EAPC_SINR_HeNB2 - SINR_target;

% EAPC power control codes
   if SINR_HeNB1_DIFF_EAPC > 0
            EAPC_HUE_ADJ = -1;
    elseif SINR_HeNB1_DIFF_EAPC< 0
              EAPC_HUE_ADJ = 1;
```

```
    else
        EAPC_HUE_ADJ = 0;
  end
  if SINR_HeNB2_DIFF_EAPC > 0
            EAPC_HUE2_ADJ = -1;
    elseif SINR_HeNB2_DIFF_EAPC < 0
              EAPC_HUE2_ADJ = 1;
    else
        EAPC_HUE2_ADJ = 0;
  end

 % EAPC power control codes

 if SINR_eNB_DIFF_EAPC > 0
     EAPC_MUE_ADJ = -1;
    elseif SINR_eNB_DIFF_EAPC < 0
             EAPC_MUE_ADJ = 1;
    else
      EAPC_MUE_ADJ = 0;
 end

% COMPUTE QOS OF MUE/HUE
      EAPC_P_MUE = min(max(MUE_Min_P,(EAPC_P_MUE
+ (EAPC_MUE_ADJ*spv))),MUE_Max_P);
 % to ensure that transmit power (P_3) is between Min &
      Max EAPC_P_HUE1 =
min(max((EAPC_P_HUE1+(EAPC_HUE_ADJ*spv)),HUE_Min_P),HUE_Max_P)
; % to ensure that transmit power (P_3) is between Min & Max
      to ensure that transmit power (P_3) is between Min &
      Max EAPC_P_HUE2 =
min(max((EAPC_P_HUE2+(EAPC_HUE2_ADJ*0.5)),HUE_Min _P),HUE_Max_P);%
to ensure that transmit power is between Min & Max

    UPLINK_EAPC_Capacity_eNB = lf*BW*log2(1 + UPLINK_EAPC_SINR_eNB);
% COMPUTE CAPACITY OF MACROCELL AND FEMTOCELL
% computation of Avg cpacity of Macrocell network (sum/no)
    UPLINK_EAPC _Avg_Capacity_Macro = UPLINK_EAPC_Capacity_eNB/
Number_of_eNB;
    UPLINK_EAPC_MACRO_ARRAY{x}= UPLINK_EAPC_Avg_Capacity_Macro ;

  % COMPUTE CAPACITY OF EACH HeNBs
 % CAPACITY BASED ON EAPC
    UPLINK_EAPC_Capacity_HeNB1 = lf*BW*log2(1 +
UPLINK_EAPC_SINR_HeNB1);
    UPLINK_EAPC_Capacity_HeNB2 = lf*BW*log2(1 +
UPLINK_EAPC_SINR_HeNB2);

% ARRAY OF THROUGHPUT
EAPC_eNB_THROUGHPUT_ARRAY{x}= UPLINK_EAPC_Capacity_eNB;
EAPC_HeNB1_THROUGHPUT_ARRAY{x}= UPLINK_EAPC_Capacity_HeNB1;
EAPC_HeNB2_THROUGHPUT_ARRAY{x}= UPLINK_EAPC_Capacity_HeNB2;
UPLINK_EAPC_FM_ARRAY{x}= EAPC_eNB_THROUGHPUT_ARRAY{x} +
EAPC_HeNB1_THROUGHPUT_ARRAY{x}+EAPC_HeNB2_THROUGHPUT_ARRAY{x};

% COMPUTE UPLINK CAPACITY OF FEMTOCELL
% computation of Avg capacity of femto
    UPLINK_EAPC_Avg_Capacity_Femto =(UPLINK_EAPC_Capacity_HeNB1
+ UPLINK_EAPC_Capacity_HeNB2)/Number_of_HeNB ;
   UPLINK_PC1_Avg_Capacity_Femto = (UPLINK_PC1_Capacity_HeNB1 +
    UPLINK_EAPC_FEMTO_ARRAY{x}= UPLINK_EAPC_Avg_Capacity_Femto ;
```

```
% average power consumption
   % power consumption
   EAPC_HUE_P_ARRAY{x} =(EAPC_P_HUE1
   +EAPC_P_HUE2)/Number_of_HeNB; EAPC_MUE_P_ARRAY{x} = EAPC_P_MUE
end

% AVERAGE  THROUGHPUT
EAPC_MUE_THR_SUM = (EAPC_MUE_THROUGHPUT_ARRAY{1}+
EAPC_MUE_THROUGHPUT_ARRAY{2}+EAPC_MUE_THROUGHPUT_ARRAY{3}+EAPC_MUE_THR
OUGHPUT_ARRAY{4}+EAPC_MUE_THROUGHPUT_ARRAY{5}+EAPC_MUE_THROUGHPUT_ARRA
Y{6}+
EAPC_MUE_THROUGHPUT_ARRAY{7}+EAPC_MUE_THROUGHPUT_ARRAY{8}+EAPC_MUE_THR
OUGHPUT_ARRAY{9}+EAPC_MUE_THROUGHPUT_ARRAY{10});

% MUE CAPACIITY bar chart analysis
      EAPC_MACRO_THROUGHPUT_bar= [EAPC_MACRO_THROUGHPUT_ARRAY{1};
EAPC_MACRO_THROUGHPUT_ARRAY{2};EAPC_MACRO_THROUGHPUT_ARRAY{3};
EAPC_MACRO_THROUGHPUT_ARRAY{4};
EAPC_MACRO_THROUGHPUT_ARRAY{5};EAPC_MACRO_THROUGHPUT_ARRAY{6};
EAPC_MACRO_THROUGHPUT_ARRAY{7};EAPC_MACRO_THROUGHPUT_ARRAY{8};
EAPC_MACRO_THROUGHPUT_ARRAY{9}; EAPC_MACRO_THROUGHPUT_ARRAY{10}];
   PC1_MACRO_THROUGHPUT_bar = [PC1_MACRO_THROUGHPUT_ARRAY{1};

% HUE throughput bar chart analysis

   EAPC_FEMTO_THROUGHPUT_bar = [EAPC_FEMTO_THROUGHPUT_ARRAY{1};
EAPC_FEMTO_THROUGHPUT_ARRAY{2};EAPC_FEMTO_THROUGHPUT_ARRAY{3};
EAPC_FEMTO_THROUGHPUT_ARRAY{4};
EAPC_FEMTO_THROUGHPUT_ARRAY{5};EAPC_FEMTO_THROUGHPUT_ARRAY{6};
EAPC_FEMTO_THROUGHPUT_ARRAY{7};EAPC_FEMTO_THROUGHPUT_ARRAY{8};
EAPC_FEMTO_THROUGHPUT_ARRAY{9}; EAPC_FEMTO_THROUGHPUT_ARRAY{10}];
   PC1_FEMTO_THROUGHPUT_bar = [PC1_FEMTO_THROUGHPUT_ARRAY{1};
y_HUE_THROUGHPUT =
[abs(APC_FEMTO_THROUGHPUT_bar),abs(EAPC_FEMTO_THROUGHPUT_bar),abs(PC1_
FEMTO_THROUGHPUT_bar)]
% HUE SINR

     EAPC_HUE_SINR_bar = [EAPC_HUE_SINR_ARRAY{1};
EAPC_HUE_SINR_ARRAY{2};EAPC_HUE_SINR_ARRAY{3};EAPC_HUE_SINR_ARRAY{4};E
APC_HUE_SINR_ARRAY{5};EAPC_HUE_SINR_ARRAY{6};
EAPC_HUE_SINR_ARRAY{7};EAPC_HUE_SINR_ARRAY{8};EAPC_HUE_SINR_ARRAY{9};E
APC_HUE_SINR_ARRAY{10}];

% eNB AVERAGE POWER  CONSUMPTION
      EAPC_eNB_P_bar =[(EAPC_eNB_P_ARRAY{1}+
EAPC_eNB_P_ARRAY{2}+EAPC_eNB_P_ARRAY{3}+EAPC_eNB_P_ARRAY{4}+EAPC_eNB_P
_ARRAY{5}+EAPC_eNB_P_ARRAY{6}+
EAPC_eNB_P_ARRAY{7}+EAPC_eNB_P_ARRAY{8}+EAPC_eNB_P_ARRAY{9}+EAPC_eNB_P
_ARRAY{10})/(Number_of_loop);0];

Y_eNB_Power = [APC_eNB_P_bar,EAPC_eNB_P_bar,PC1_eNB_P_bar]
UPLINK_MACRO_y =
[abs(UPLINK_APC_MACRO_bar),abs(UPLINK_EAPC_MACRO_bar),abs(UPLINK_PC1_M
ACRO_bar)]

UPLINK_FEMTO_y =
[abs(UPLINK_APC_FEMTO_bar),abs(UPLINK_EAPC_FEMTO_bar),abs(UPLINK_PC1_
F EMTO_bar)]
```

```
% eNB_HeNB bar chart
   analysis UPLINK_FM_y =
[abs(UPLINK_APC_FM_bar),abs(UPLINK_EAPC_FM_bar),abs(UPLINK_PC1_FM_bar) ]

% MUE POWER CONSUMPTION

Y_MUE_P = [APC_MUE_P_bar,EAPC_MUE_P_bar,PC1_MUE_P_bar]
% HUE POWER CONSUMPTION
Y_HUE_P = [APC_HUE_P_bar,EAPC_HUE_P_bar,PC1_HUE_P_bar]
% cdf plot
% sort command arrange the datas (eNB throughput) in ascending order
                UPLINK_x1_EAPC_MACRO =sort(abs(UPLINK_EAPC_MACRO_bar))
        UPLINK_EAPC_M= ceil(mean(UPLINK_x1_EAPC_MACRO))
        UPLINK_EAPC_s= ceil(std(UPLINK_x1_EAPC_MACRO))
% eNB OBJECT OF DISTRIBUTION
        UPLINK_EAPC_PD =
makedist('Normal','mu',UPLINK_EAPC_M,'sigma',UPLINK_EAPC_s)
        UPLINK_PC1_PD =
        HeNB_eNB_x_axis =0:5:60
        HeNB_x_axis  = 0:5:60;
        eNB_x_axis  = 0:5:60;

% y component in cdf for HeNB throughput
        UPLINK_cdf_normal_EAPC_FEMTO =
cdf(UPLINK_EAPC_FPD,HeNB_x_axis)
% y component in cdf for eNB throughput
        UPLINK_cdf_normal_EAPC_MACRO = cdf(UPLINK_EAPC_PD,eNB_x_axis)

Y_HeNB_Power = [APC_HeNB_P_bar,EAPC_HeNB_P_bar,PC1_HeNB_P_bar]

x_axis_macro_throu  = 0:5:60;
x_axis_femto_throu  = 0:5:60;

figure (1) % macrocell power
    bar(Y_eNB_Power)
    title('Benchmark Average en-gNB Transmit Power
    ','FontSize',9); xlabel('Power Technique','FontSize',10)
    ylabel('en-gNB Average Power Consumption
(dBm)','FontSize',10) grid on
    legend('APC','EAPC','PC1')
    legend('APC','EAPC','PC1')

figure(5) % Femto throughput
    DOWNLINK_J_FEMTO =
plot(x_axis_femto_throu,DOWNLINK_cdf_normal_APC_FEMTO,'-*k');
    title('Benchmark of HUE throughput
    ','FontSize',10); xlabel('Throughput
    (Mbps)','FontSize',10) ylabel('CDF','FontSize',10)
grid on
  hold on;
    DOWNLINK_K_FEMTO =
plot(x_axis_femto_throu,DOWNLINK_cdf_normal_EAPC_FEMTO,'-or');
    DOWNLINK_L_FEMTO =
plot(x_axis_femto_throu,DOWNLINK_cdf_normal_PC1_FEMTO,'-g*');
    legend([DOWNLINK_J_ FEMTO DOWNLINK_K_FEMTO
DOWNLINK_L_FEMTO ],'APC','EAPC','PC1');

hold off;
```

APPENDIX B (Publication)

Dawar, K. P., Usman, A. U., & Salihu, B. A. (2021). An Enhanced Active Power Control Technique for Interference Mitigation in 5G Uplink Macro-Femto Cellular Network. *IEEE International Conference on cyberspace (CYBER NIGERIA)*, 2, 85-90.